The Dynamic Behavior of Domain Walls in Barium Titanate

Technical Report 87
Laboratory for Insulation Research
Massachusetts Institute of Technology

October, 1954

The Dynamic Behavior of Domain Walls in Barium Titanate

by

Elizabeth A. Little

Laboratory for Insulation Research
Massachusetts Institute of Technology
Cambridge, Massachusetts

O. N. R. Contract N5ori-07801

October, 1954

THE DYNAMIC BEHAVIOR OF DOMAIN WALLS IN BARIUM TITANATE*

by

Elizabeth A. Little †

Laboratory for Insulation Research
Massachusetts Institute of Technology
Cambridge, Massachusetts

Abstract: The nucleation and growth of 180° (antiparallel) domains and 90° domains in barium titanate single crystals have been measured with optical techniques.

The creation of 180° domains proceeds by the nucleation of long thin spikes with an initial velocity along the polar axis of about 10^4 cm/sec. for E = 5 kv/cm. As neutralizing electric charges accumulate at the domain walls, the spikes widen to form wedge-shaped domains and the total switching time is determined by the slow growth velocity of such space-charge-compensated wedges. The limiting field for 180° domain growth is nearly identical with the limiting field for nucleation of a domain.

The growth of 90° domains in an electric field also begins by the nucleation of long thin wedges. Direct measurements of the nucleation rate as a function of time and field strength show that this rate traverses a maximum as a function of time. The maximum growth rate of a single wedge approaches asymptotically about 10^6 cm/sec. with increasing field strength. After a 90° domain has been introduced into a single-domain crystal, its growth may be described in terms of the sideways motion of 90° walls. The critical field for wall motion is considerably smaller than

---

* Based on a thesis submitted in partial fulfillment of the requirements for the degree of Doctor of Philosophy in Physics at the Massachusetts Institute of Technology.

† IBM Fellow.

that for domain nucleation. The displacement of a 90° wall is strongly dependent on strains and the state of clamping of the crystal, and wall motion appears to cease for frequencies in the megacycle range, where the piezoelectric resonances of the whole crystal set in. The wall thickness is appreciably larger for the 90° than for the 180° wall.

The interaction of 90° and 180° domains has also been investigated. 90° walls may form head-to-head or tail-to-tail configurations, which can only be switched by the intermediate formation of 180° domains. Complicated interaction effects occur and lead to notably long relaxation times.

Finally, the free energy for rotation of the polar axis through 90° has been calculated and an approximate value for the energy of a 90° wall derived.

Introduction

First reported in 1942 by Wainer and Salomon[1] as having unusual dielectric characteristics, barium titanate revealed uncommon electrical, mechanical and optical properties in rapid succession. Investigations performed at the Laboratory for Insulation Research by von Hippel and co-workers[2, 3] and shortly thereafter in Russia by Wul and co-workers[4], established barium titanate as a new ferroelectric material. At the Curie point near 120°C, a phase transition

1) E. Wainer and A. N. Salomon, Titanium Alloy Mfg. Co. Elect. Rep. 8 (1942), 9 and 10 (1943).

2) A. R. von Hippel and co-workers, N.D.R.C. Rep. No. 300, Aug., 1944; 540, Oct., 1945.

3) A. R. von Hippel, R. G. Breckenridge, F. G. Chesley, and L. Tisza, Ind. Eng. Chem. 38, 1097 (1946).

4) B. M. Wul and I. M. Goldman, Compt. rend. (USSR) 46, 139 (1945); B. M. Wul and L. F. Vereshchagin, Compt. rend. (USSR) 48, 634 (1945).

from cubic to tetragonal occurs[5] and hysteresis loops develop; at room temperature the c/a ratio has reached about 1.01. Two additional phase transitions are observed near 0° and -80°C.[2, 3] The ceramic when prepolarized, is strongly piezoelectric.[6]

With the discovery of a method of growing good crystals from ternary melts[7, 8], measurements on single crystals were made possible. The several phases can be characterized as follows.[9, 10] Above 120°C the crystal is cubic with no spontaneous polarization. Below 120° a spontaneous polarization P_s of about 0.26 coul/m^2 develops.* From 120° to 0°C, P_s is directed along a ⟨100⟩ direction, from 0° to -80°C along a ⟨110⟩ direction, and below -80°C along a ⟨111⟩ direction of the original cube. In each case the mechanical deformation of the lattice is proportional to the square of the polarization: expansion takes place in the direction of the polarization and contraction at right angles to it. It follows that as the temperature is lowered from above 120°C, the crystal symmetry changes successively from cubic, O_h, to tetragonal, C_{4v}, to orthorhombic, C_{2v}, to rhombohedral, C_{3v}.[11]

In the tetragonal phase with which the present study is concerned, the optical ellipsoid is uniaxial negative[9] and the birefringence, $n_c - n_a$, where n_c

5) H. D. Megaw, Proc. Roy. Soc. (London) 189A, 261 (1947); Trans. Faraday Soc. 42A, 224 (1946).

6) S. Roberts, Phys. Rev. 71, 890 (1947).

7) H. Blattner, B. Matthias and W. Merz, Helv. Phys. Acta 20, 225 (1947).

8) H. Blattner, B. Matthias, W. Merz and P. Scherrer, Experientia 3, 148 (1947).

9) P. W. Forsbergh, Jr., Phys. Rev. 76, 1187 (1949).

10) W. J. Merz, Phys. Rev. 76, 1221 (1949).

* MKS units will be used.

11) H. F. Kay and P. Vousden, Phil. Mag. [7] 40, 1019 (1949).

and n_a are the indices of refraction along the a and c axes, respectively, is proportional to the mechanical deformation.[9,10] The birefringence is about - 0.055 for sodium light at room temperature.

The dielectric constants of single domain crystals for fields applied in the c and a directions have been measured by Merz.[10] The susceptibilities at room temperature are $\chi_a = 5000$ and $\chi_c = 300$ (where $\chi = \epsilon/\epsilon_o - 1$). Measurements of the dielectric constant as a function of frequency have indicated a relaxation commencing in the ceramic at about 10^8 cycles.[12,13]

In the perovskite structure of barium titanate, the barium ions are at the corners, oxygen ions at the face centers and titanium ions at the body center of the simple cubic unit cell. The spontaneous polarization is generally considered to be associated with the displacement of the titanium ions from the center of the original cube. As von Hippel[14] has suggested, to explain the existence of a spontaneous polarization, both ionic and covalent bonding must be invoked and a feedback effect introduced correlating the motions of the titanium and oxygen ions. Slater[15] has shown that the Lorentz field at the titanium ion, enhanced by the presence of the (1/2, 1/2, 0) and (1/2, 1/2, 1) oxygen ions, is more than enough to account for a spontaneous polarization. Devonshire[16] has advanced an "interaction" equation which is useful for correlating experimental parameters. Before a final molecular theory can be formulated, more detailed experimental

---

12) J. G. Powles and W. Jackson, Proc. Inst. Elect. Engrs. 96, Pt. 3, 383 (1949).

13) A. R. von Hippel and W. B. Westphal, National Research Council Conference on Electrical Insulation, October, 1948.

14) A. R. von Hippel, Revs. Mod. Phys. 22, 221 (1950).

15) J. C. Slater, Phys. Rev. 78, 748 (1950).

16) A. F. Devonshire, Phil. Mag. [7] 40, 1040 (1949); 42, 1065 (1951).

information is needed.

After Matthias and von Hippel[17] discovered the existence of domains in the ferroelectric phases of barium titanate, Forsbergh[9] described the observed domain geometry in detail. 90° domains are regions of uniform polarization formed in the tetragonal phase by twinning on $\{101\}$ planes of the crystal. That the optical axis changes by 90° across a domain boundary can be verified with a quarter-wave plate. "90° walls", as these twin planes will hereafter be called, are visible because of the distortion at the wall. Such domains are introduced into a crystal by the advance of thin wedges.[9,17]

Recently it has been shown by optical means that there also exist domains formed by $\{100\}$ twin planes.[18,19] Since there is normally no distortion at such a twin plane (180° wall) and a polar-axis change of 180° can not be detected by either optical or X-ray techniques, the existence of these antiparallel domains was originally concluded by indirect evidence from distorted hysteresis loops.[10,14]

The initial polarization curve of barium titanate, the dielectric nonlinearity, hysteresis loops and their frequency dependence are to a large extent caused by the generation, motion, and interaction of domains. In contrast to the opaque ferromagnetic materials, where domain effects can be studied only at the surface by the Bitter technique, the transparent ferroelectrics allow an optical investigation throughout the volume by birefringence observations. In this way, static domain patterns as well as domain dynamics can be followed in all details and the electrical characteristics of the material interpreted by unambiguous

---

17) B. Matthias and A. von Hippel, Phys. Rev. 73, 1378 (1948).

18) W. J. Merz, Phys. Rev. 88, 421 (1952).

19) L. E. Cross, A. T. Dennison and M. M. Nicolson, Leeds Philosophical and Literary Soc. (Sci. Section) 5, Pt. 3, 199 (1949).

optical evidence. This knowledge is needed for an understanding of the operation, possibilities and limitations of ferroelectric devices like transducers, memory devices and dielectric amplifiers. The present study on the dynamics of domain walls is a first installment to acquire this knowledge.

After this study was finished, the author received a prepublication copy of work done by Merz[20] on the switching of 180° domains. The domain velocity determined from the switching time agrees well with the value we find here using optical techniques. It is interesting that a relation he finds between the field strength and the nucleation rate of 180° domains occurs also for the 90°-domain nucleation process.

Experimental Procedures

Preparation of Crystals

The plate crystals used in these experiments were grown from ternary melts following the method of Matthias et al.[7,8] The variation chosen provided a maximum yield of thin "a" crystals, for which the polar axis lies in the crystal plane ("c" crystals, in contrast, have their polar axis perpendicular to the crystal plate).

Fifty grams of $BaCl_2$, 25 g of $BaCO_3$ and 5 g of TiO_3, ground together in a mortar, were heated in an alundum crucible in 1/2 h. to 1400°C, held at this peak temperature for 1 h. and then cooled (in 1 h. to 1200°, in 5 h. to 900°C). After dissolving the $BaCl_2$ flux in water, the single-domain "a" crystals were selected by microscopic inspection. The crystals thus obtained are about 10 μ thick and 400x400 μ^2 in area. Because of the thinness of the sample, most domain patterns varied in only two dimensions, that is, extended through the thickness of the crystal.

To provide electrodes, the crystal was laid flat on a microscope slide

20) W. J. Merz, private communication, June, 1954; Phys. Rev. 95, 690 (1954).

and, by using a micromanipulator, Dupont silver paint No. 4548 was spread along the glass and onto two opposite edges of the crystal. We will call the "a" crystals [100], [001], or [101] crystals, if the electrodes are attached to [100], [001] or [101] edges, respectively.

Microscopic Techniques

Because of the birefringence of barium titanate, the polarizing microscope is the ideal tool for a study of domain structure. Viewed along the polar axis, a domain appears black under crossed Nicols. Viewed perpendicular to the polar axis, as in the case of "a" crystals, a domain will transmit light unless the light is polarized parallel to the "c" or "a" axis. In the latter conditions the domain is oriented at extinction.

Since the mechanical, electrical, and optical axes are related, the extinction direction will be rotated if the crystal is distorted electrically or mechanically. By observing the rotation of the extinction direction in an electric field, the uniformity of the field and the existence of strains in the crystal can be studied. The optical magnification here used ranged up to 1100X.

A micrometer eyepiece and a Land camera served for most observations. For fast processes a 16 mm Cine-Kodak movie camera with frame speeds up to 64 per second was used. Wall movements down to 1/2 μ could be measured on a standard microfilm viewer. A carbon arc lamp with a water filter provided a high intensity light source.

Electrical Instrumentation

A small furnace on the microscope stage allowed observations up to 150°C. To provide various types of electric fields, several power supplies were used. Short, rectangular pulses of from 10 to 200 μsec. duration could be produced by the pulse generator of Fig. 1a. For pulses 1/4 to 3 μsec., the circuit shown in Fig. 1b was employed. The rise and decay time of the pulses proved negligible

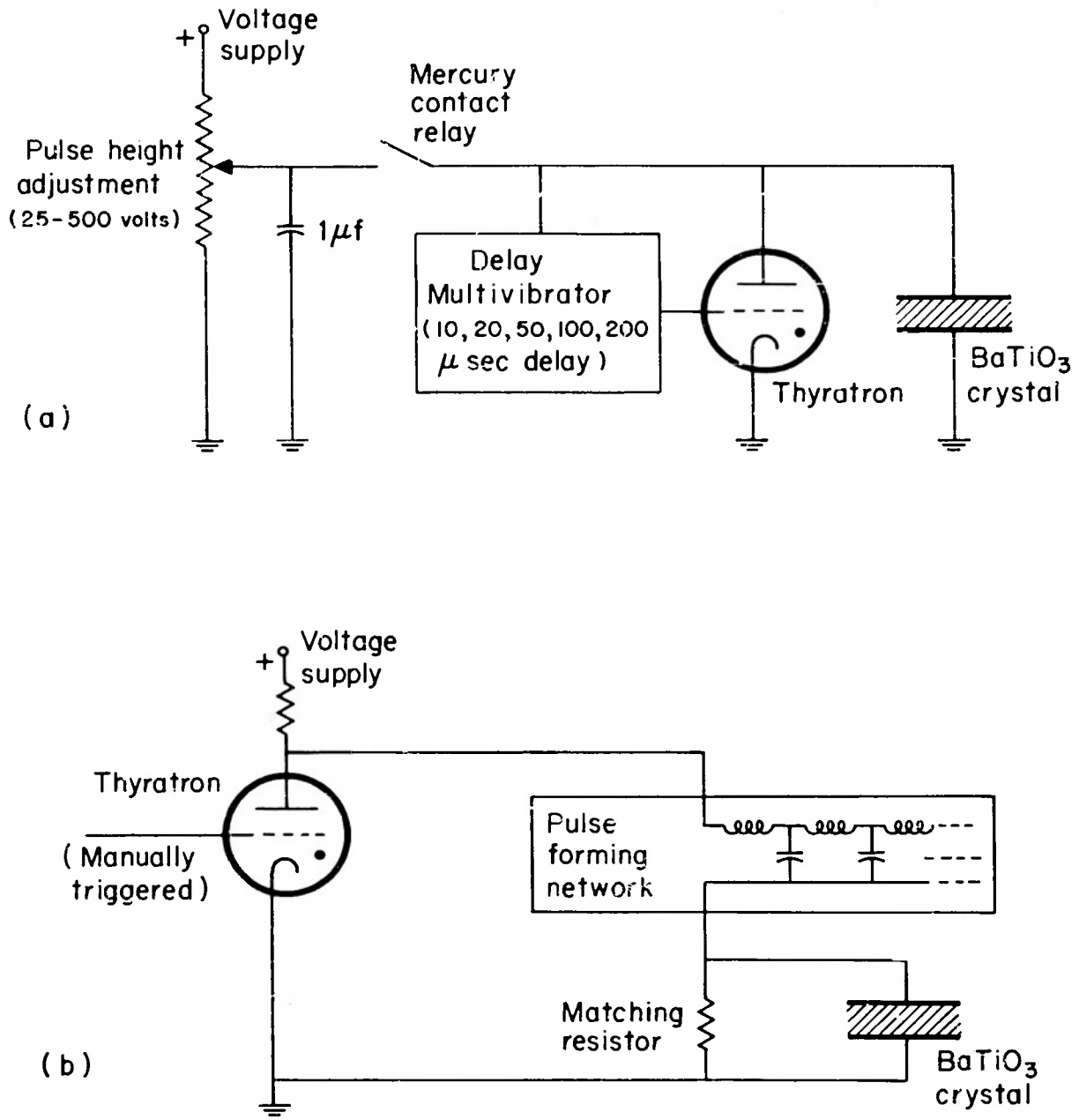

Fig. 1. Rectangular pulse generator circuits.

compared to the pulse length except for the 1/4 μsec. pulses which were slightly bell-shaped. The width of such a pulse at 70 percent of its height was 1/4 μsec.

For rectangular pulses of the order of seconds or longer a toggle switch connecting to "B" batteries was employed. A-c fields were provided by a standard low frequency generator ranging from 10^{-2} to 10^{3} cps (also used for square waves); by an audio oscillator covering the range from 20 to 20,000 cps; and by a bridge oscillator giving the selected frequencies: 30, 70, and 300 kcps.

Antiparallel Domains

In a "c" crystal or a [001] "a" crystal, a field opposite to the polar axis will favor the creation and growth of antiparallel domains. However, since there is normally no observable distortion at 180° walls at magnifications up to 1100X, antiparallel domains in such crystals are not visible. Mertz[18] first made 180° domains visible by applying an electric field normal to the c axis. The polar axes in adjacent antiparallel domains are here rotated in opposite directions and differ in their extinction positions (Fig. 2). For an optical study of the dynamic behavior of 180° walls, thin "a" crystals with [101] edges are therefore uniquely suited. One component of the field makes the domains visible, the other forces them to grow. If not very large fields are applied, additional formation of 90° domains can be avoided. Figure 3 shows such a [101] crystal with its antiparallel domains: the domains of one polarity are in extinction (black), those of opposite polarity transmit light. One can observe that a transition region of about 1/2 micron width at the wall does not rotate in the field.

Nucleation and Initial Motion

To study the initial growth of 180° domains, short rectangular pulses were applied to a single domain crystal. (The field strength will be designated as negative when opposite to the initial polarization.)

A negative pulse of 7.4 kv/cm (length 200 μsec.) applied to a single domain crystal at extinction causes normally only a barely perceptible flash of light. Reversal of the field direction shows nothing different. We cannot say assuredly that no domains were introduced, but certainly no permanent domains were formed. With continuous pulsing, occasionally some thin (1/2 to 5 μ at the widest part) spikes appear, extending from an edge nearly across the crystal (0.05 cm); they remain visible for as long as a second after pulsing. For as many as 50 subsequent pulses these same wedges have been observed; they do not appear to grow. If the field is reversed, the first

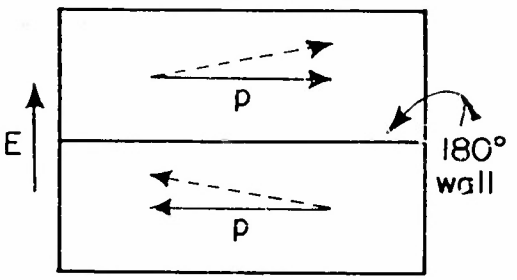

Fig. 2. Rotation of polar axes near a 180° wall in a field perpendicular to the wall.

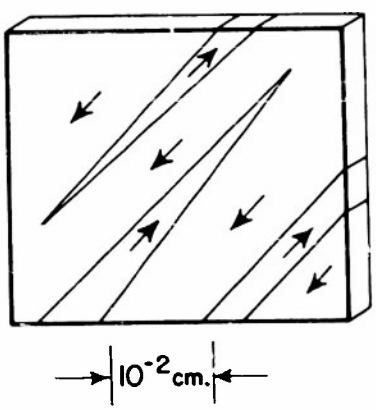

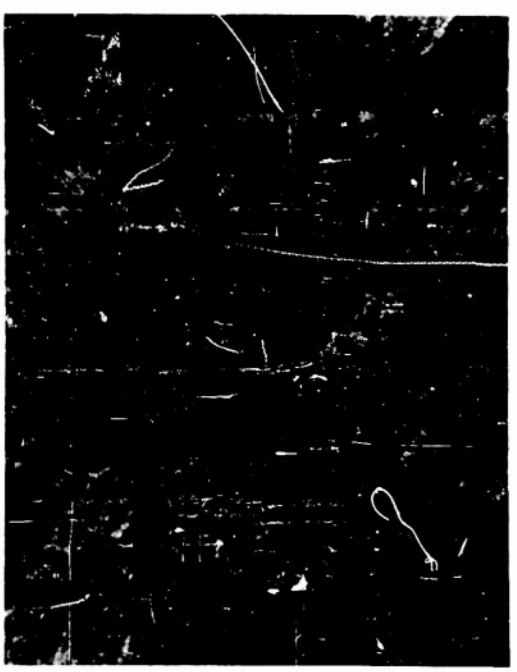

Fig. 3. 180° domains in a [101] crystal.

pulse will reveal for about a second the same wedges, shortened to about 0.01 cm.

No wedges were observed to form for pulses shorter than 10 μsec. in fields up to 11 kv/cm or, for pulses shorter than 200 μsec. up to 7 kv/cm. (A spike thinner than 0.5 μ would not be visible.)

Additional information was obtained by performing an inverse experiment. A few large (20 μ wide and 500 μ long) antiparallel domains were introduced into the crystal by a low negative d-c field. These wedges, left undisturbed, will remain in the crystal for 24 h. or longer. Short positive pulses (E = 7.5 kv/cm), spaced several seconds apart, were applied to remove the wedges, and the number of required pulses recorded as a function of pulse length (Fig. 4). As each pulse is applied, the domains still present become visible for about a second. If the pulse rate is increased, more pulses are required for the removal of the wedges.

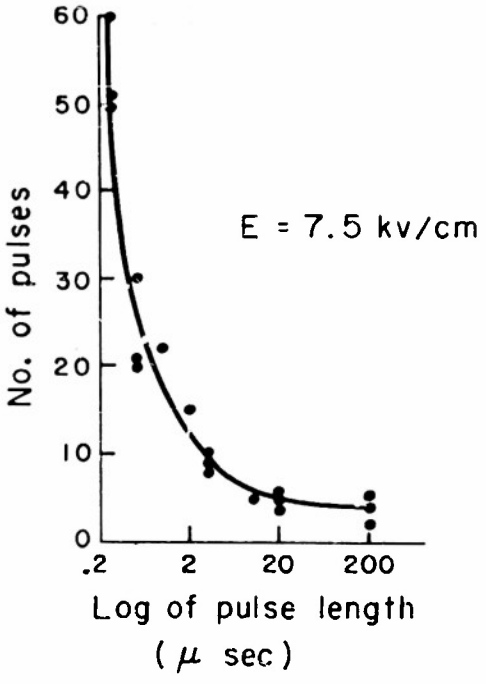

Fig. 4. Number of pulses required to remove 180° domains as a function of pulse length.

When pulses of 10 μsec. or longer are used, some domains are removed entirely by the first pulse; a bright region left behind fades out in about a second. For pulses shorter than 1 μsec., each pulse narrows the domains significantly and the wedge tip retreats slightly.

Discussion

Two tentative conclusions can be drawn from these experiments: 1) The formation of an antiparallel domain begins as a spike at the edge of the crystal; it extends along the polar axis with a velocity between 5×10^3 and 5×10^4 cm/sec.

at 7.5 kv/cm. 2) Space-charge effects appear associated with the stabilization of the wedges; their relaxation time in our crystals is of the order of a second.

This second conclusion, based on the visible aftereffects of pulses, requires a closer examination. If a 180° domain is wedge-shaped with a wedge angle θ, the saturation polarization P_s produces a large electric field, $\sim (P_s/\epsilon_o) \sin\theta \sim 10^5 \sin\theta$ kv/cm, at the walls, caused by the free ends of the dipole chains. Such a field should create a large lattice distortion near the 180° wall, but quasi-stationary domains with a wedge angle of 20° or more do not show such distortions. This suggests that a compensating electric charge accumulates and neutralizes the ends of the dipole chains.

Since the initial wedge velocity is high and the relaxation time of the free charge (fading of the bright region) is of the order of a second, the space charge is not able to follow the domain-wall motion during the initial propagation of a 180° domain. Thin domains without appreciable wedge angle might be nucleated and removed by short pulses. As soon as compensating charges can accumulate on domain walls, domains are stabilized.

This concept receives support from the experiment which measures the number of pulses required to remove domains (Fig. 4). The curve found can be expressed by

$$N = 28 \ln \frac{t_o}{t} \quad , \tag{1}$$

where t is the pulse length and t_o equals 0.15 μsec. The increase in the required number of pulses with decreasing time becomes understandable if the domain-wall velocity decreases as it leaves its space charge behind. Many short pulses spaced by intervals of several seconds allow the space charge to catch up and prove to be therefore more effective in removing domains than a few long pulses, as long as the pulse length is short in comparison to the time constant of the space-charge motion.

These experiments are in line with the concept of von Hippel[21] that the conductivity of $BaTiO_3$ crystals is of great importance for the dynamics of the domain formation, and with observations by Mitsui and Furuichi[22] on the effect of charges on the domains in Rochelle salt crystals.

Reversal of the Saturation Polarization by Antiparallel Domains

The manner in which spikes widen and lengthen in a negative d-c field until the crystal polarization is reversed, is illustrated schematically in Fig. 5.

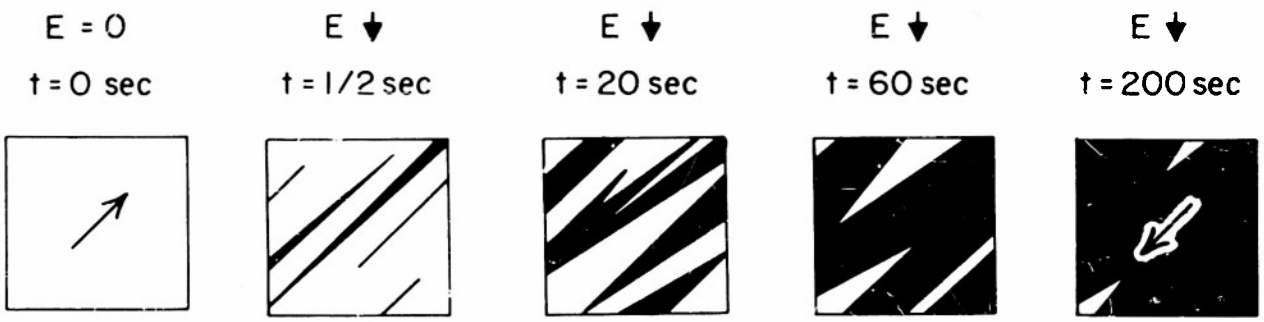

Fig. 5. Schematic diagram of 180° domain-switching process in [101] crystals.

The last domains to leave are wide wedges at the edges of the crystal; they are often difficult to remove completely even with a high field.

To study these slow processes and avoid the formation of 90° wedges, a negative field is applied gradually to a single-domain crystal, reaching its peak field strength E in about 1/2 sec. Typical thin spikes starting from both directions extend across the crystal before E is reached. These spikes tend to nucleate at identical places at the edge of the crystal when the experiment is repeated. The number of such spikes, which increases with E as well as with the time derivative of the field, is plotted against E in Fig. 6. The times required to reach approximately 50 (a) or 90 percent (b) reversal are shown as a function

21) A. R. von Hippel, Tech. Rep. 51, Lab. Ins. Res., Mass. Inst. Tech., March, 1952.

22) T. Mitsui and J. Furuichi, Phys. Rev. 90, 193 (1953).

of the peak field strength in Fig. 7 (the areas of opposite polarity were estimated visually). Since 1/t is related to the velocity of reversal, this parameter has also been plotted in Fig. 7 in its dependence on E.

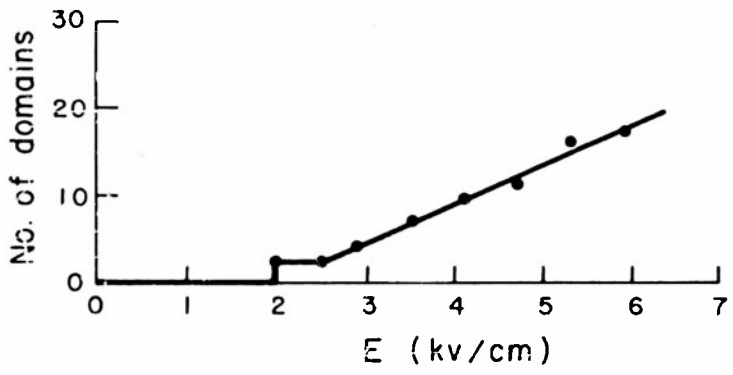

Fig. 6. Number of 180° domains nucleated in a d-c field as a function of field strength.

The characteristics show that a minimum field strength of about 2 kv/cm is required for the nucleation of the wedges. In fields smaller than 2 kv/cm, no wedges are formed during the observation period of 24 hours. For E smaller than about 2.4 kv/cm, the wedges do not grow for times as long as 12 hours. Therefore, in our [101] crystals the limiting field E_c for nucleation and growth of antiparallel domains is nearly the same. The growth velocity is slowed down appreciably in the last stages of reversal.

The shape of the curves (Fig. 7) leads again to the interpretation that the advances of spikes, initially fast, is slowed down as the electrostatic energy of the depolarizing field increases and that growth continues as a neutralizing charge accumulates on the domain walls. Therefore, we have to distinguish between two processes: the propagation of a spike with no charge compensation and the growth of a wedge with charge compensation. The time needed for 50 percent saturation will include both effects, while the time required to reverse the polarization from 50 to 90 percent should primarily reflect the growth rate of wedges with charge compensation. The number of walls present at 50 percent saturation is nearly constant for the range $3 < E < 6$ kv/cm and in this range the growth

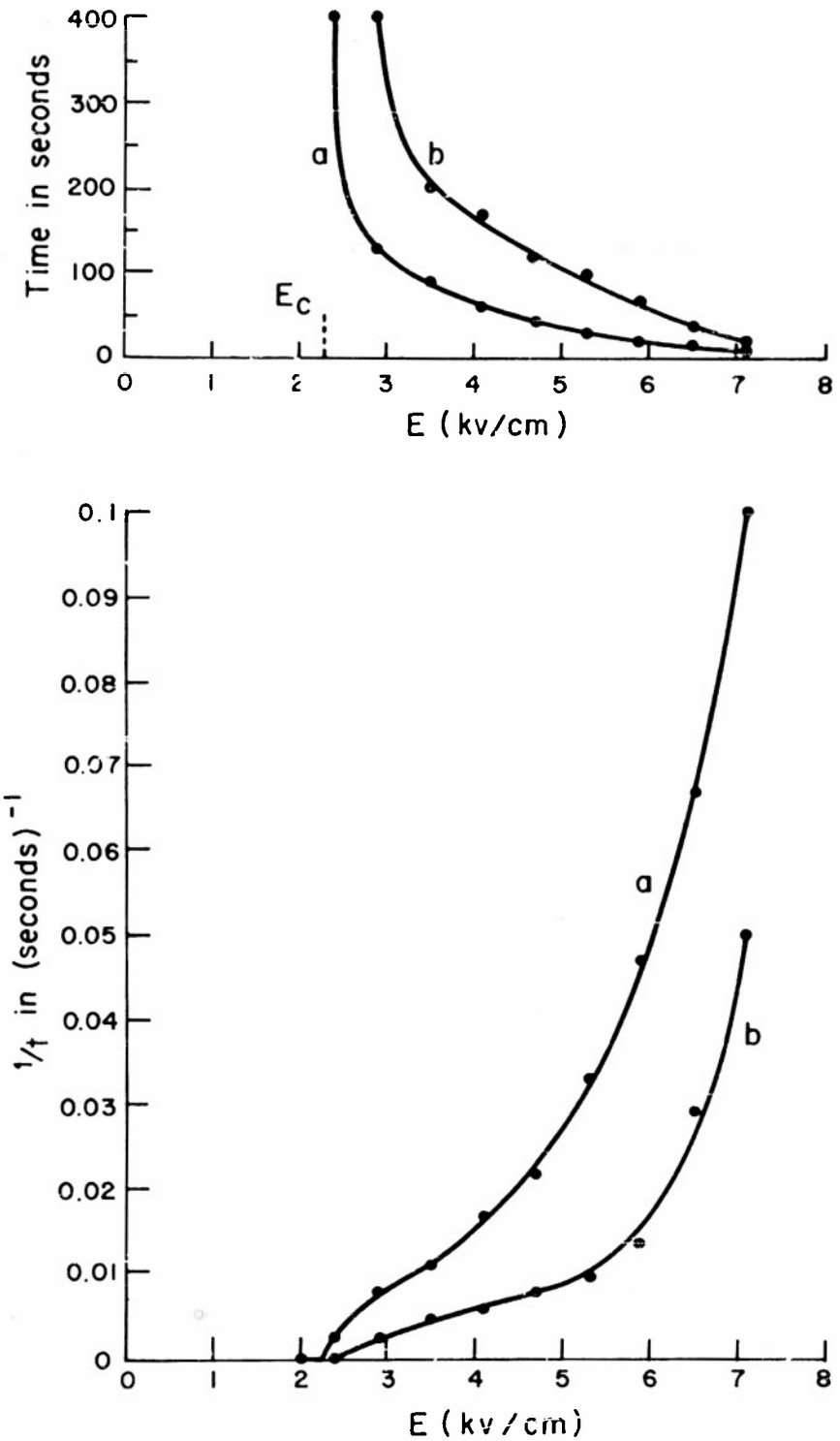

Fig. 7. Time required for 180° domains to reverse the polarization of a [101] crystal: a) by 50 percent and b) by 90 percent. Both the time and 1/time are shown as a function of d-c field strength.

velocity of wide wedges increases about linearly with $E - E_c$. Beyond 6 kv/cm, the initial, fast mechanism becomes more predominant, the slope of 1/t vs. E increases, and if E could be made large enough a crystal might be switched to opposite polarity in a very short time.

Since the 180° walls are probably quite thin (possibly only one lattice distance), motion of a 180° wall perpendicular to the polar axis should be almost impossible. The observed widening of the wedges must then be explained by a sequence of dipole flips which propagate along the polar axis (Fig. 8). The fact that about the same limiting field is observed for nucleation and growth is in line with this observation, for both processes involve the reversal of individual dipole moments.

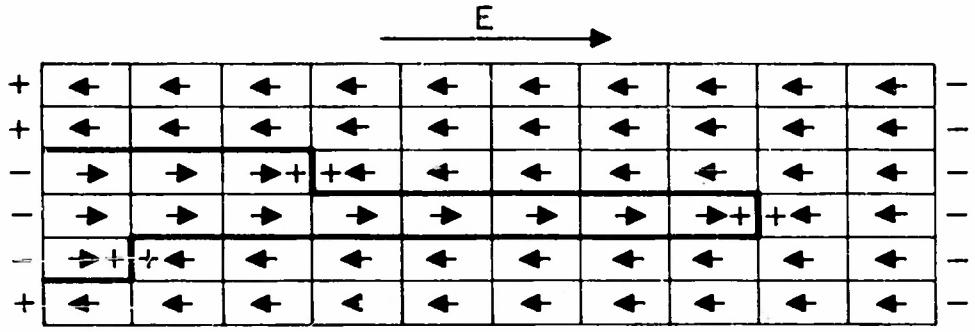

Fig. 8. Model for 180° wedge showing electrical distortions.

Temperature increase appears not significantly to change the times of reversal. However, since 90° wedges appear in great numbers at elevated temperatures and hamper the motion of 180° domains, no great significance can be attached to these results.

If one breathes on the crystal, the 180° domains move faster. Also a small photo effect appears to exist: when the arc lamp was turned off, switching seemed to take slightly longer. Both effects are consistent with the idea that the conductivity of the crystal is of importance and that we have to consider surface as well as volume conductivity.

While the results reported are common to the crystals in which we studied 180° domains, the average width and number of 180° domains seemed to vary from crystal to crystal. Since the imperfections and conductivity will very from sample to sample, this is not astonishing.

Dielectric Measurements on 180° Walls

Since the walls are not simple linear oscillators, a-c measurements are not an unambiguous tool for the study of domain dynamics, but they give important qualitative information. Figure 9a shows the susceptibility and loss tangent at high field strengths as a function of frequency for a large "c" crystal. That the wall motion damps out at around 10^4 cps is consistent with our optical results. Measurements on the tiny "a" crystals used for visual observations proved difficult because the capacitance was only of the order of tenths of micro-microfarads and the readings (especially tan δ) fluctuated widely. Figure 9b gives some measurements of χ' for such a [001] crystal. In this case, χ' is plotted against field strength with frequency as a parameter.

In both cases χ' approaches about 300 for low fields. The critical field for domain motion for the [001] crystals appears to be somewhat lower than observed visually for a [101] crystal, even when the different geometry is taken into account. This might imply that very thin and therefore invisible spikes move at low fields. That χ' increases rapidly with decreasing frequency and reaches a maximum at lower fields gives electrical evidence of the slow switching process. Hyde[23] in this laboratory found by tracing hysteresis loops that the slope $\frac{\Delta P}{\Delta E}$ continues to increase for frequencies as low as 10^{-1} cps. This would be expected from our domain observations with d-c fields.

Summary for 180° Domains

The results obtained thus far for the growth of 180° domains in a [101]

23) J. Hyde, Thesis, Mass. Inst. Tech., June, 1954.

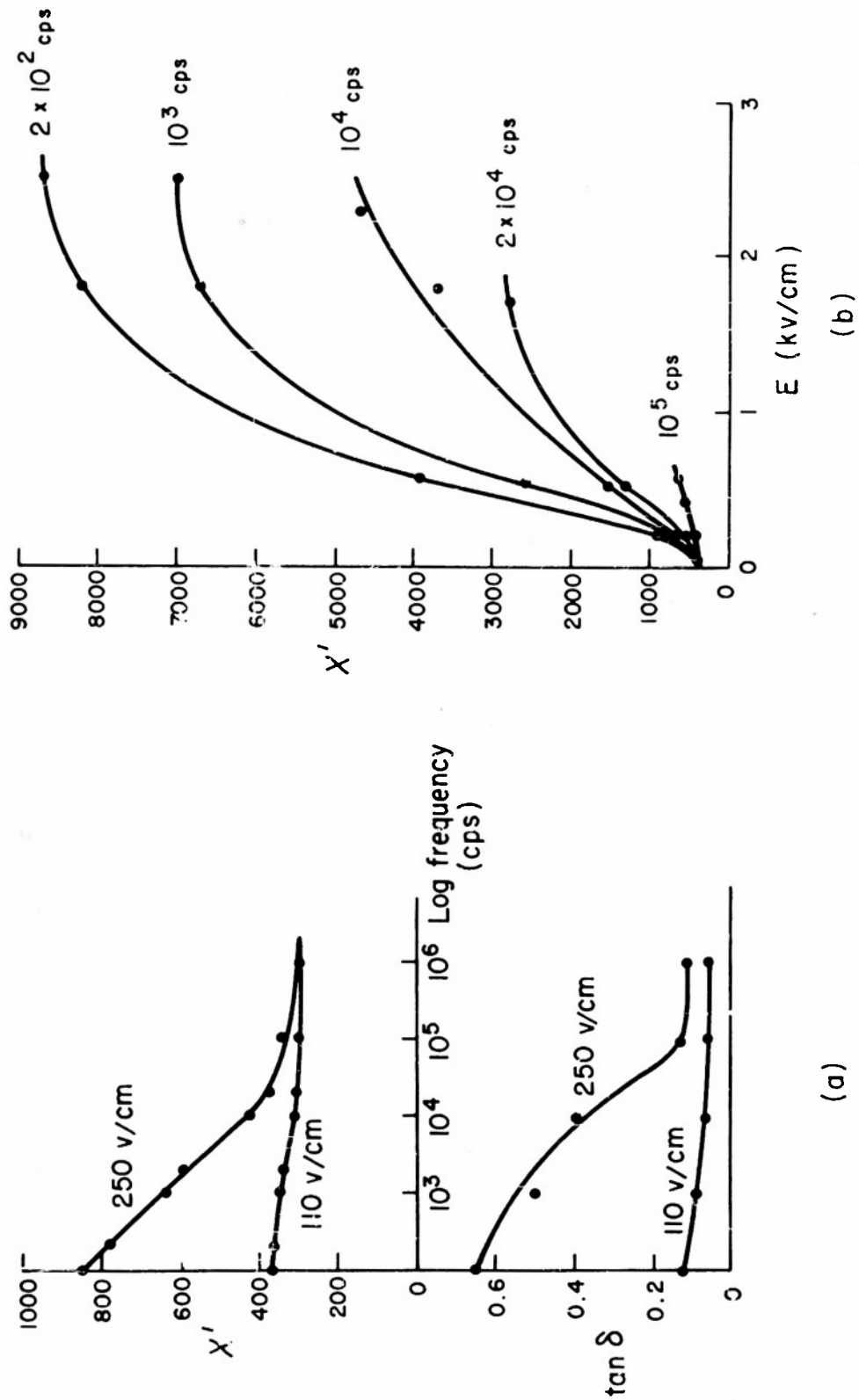

Fig. 9. Dependence of susceptibility and tan δ on field strength and frequency; (a) "c" crystal, and (b) [001] "a" crystal.

crystal might be summarized as follows. If the field strength is larger than a critical field E_c thin spikes are nucleated, probably at imperfections, and move across the crystal with a high velocity. The spikes slow down as they broaden into wedges and await the accumulation of compensating charge as they widen and eventually merge to saturate the crystal.

90° Domains

A 90° wall is a $\{101\}$ twin plane and, in contrast to 180° walls, readily visible in transmitted light as a dark line approximately 0.4 microns thick (Fig. 10). The ghosts at the edges of the line are caused by optical diffraction. (They also appear at the edges of a crystal at high magnification.) The optical axes of the domains adjacent to the 90° wall stand at an angle of 45°45' to the wall at room temperature. This is the angle corresponding to the a/c ratio of the unit cell (Fig. 10a). A 90° wall is actually an 88°30' wall, a concept of

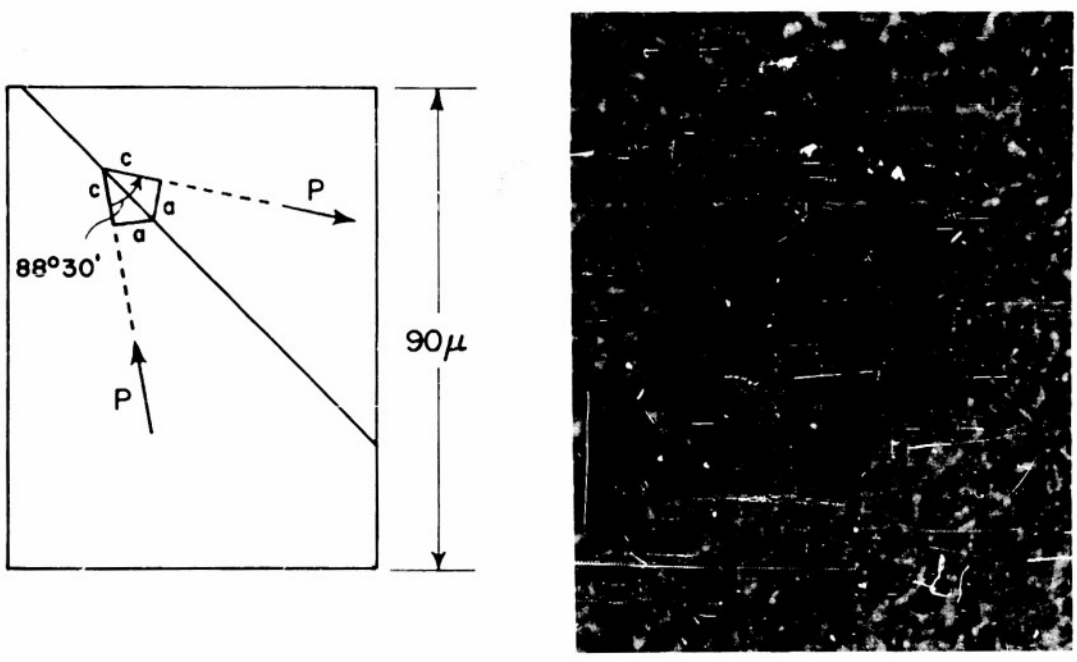

Fig. 10. 90° wall showing 1°30' distortion.

importance for the study of wall dynamics. Because of the 1^{o} 30' difference in orientation between the crystal axes across a 90^{o} twin plane, the displacement of a wall by Δx implies slip of one domain with respect to its neighbor by $\Delta y \sim \Delta x/20$ (Fig. 11). Pressure exerted on a crystal, for example by a needle, can therefore introduce and move 90^{o} domain walls.

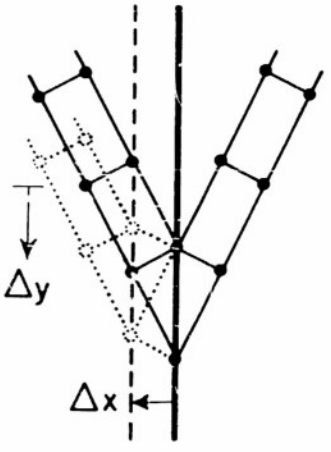

Fig. 11. 90^{o}-wall motion Δx showing corresponding slip Δy (exaggerated).

In Fig. 12 is shown a group of wedge-shaped 90^{o} domains in a pattern often found in a crystal after cooling from above the Curie point. Both the narrowness of the wedges (cf. Fig. 3), and the fact that many wedges terminate along a line, can be attributed to the mechanical distortions associated with a 90^{o} wedge.

To study 90^{o} domains without interference by 180^{o} domains, we selected a [100] crystal with the polar axis parallel to the electrodes. A good crystal of this kind is initially a single-domain crystal. A d-c field exercises in such a crystal no force tending to create antiparallel domains, but a large torque tending to rotate the polar axis by 90^{o}. If the field is increased slowly, at a critical field strength E_c, 90^{o} wedges are nucleated (Fig. 13a). The wedges, 2 to 10 μ wide, extend across the

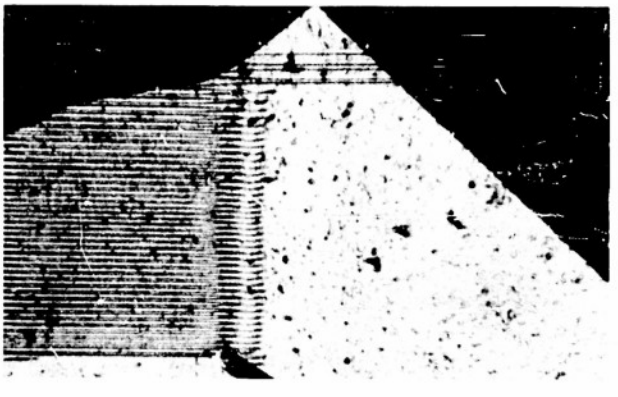

Fig. 12. A group of 90^{o} wedges in an "a" crystal.

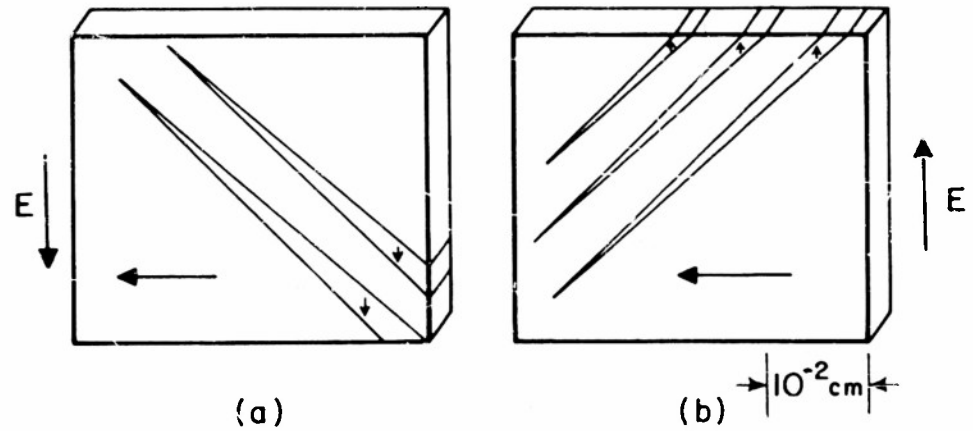

Fig. 13. 90°-wedge nucleation in a [100] crystal: a) positive field, and b) negative field.

crystal (ca. 0.05 cm) in less than 1/100 sec. If the field is removed, the stresses caused in the crystal by the presence of 90° domains may frequently force the wedges out of the crystal. They shrink slowly at first and then disappear suddenly.

In a field of opposite polarity (Fig. 13b), 90° wedges will enter from the opposite side of the crystal. Such a polarity dependence for 90° wedges (in each case they start from the cathode), was almost invariably observed in all crystals. However, there were exceptions, particularly at higher temperatures.

In Fig. 14 the electrical-mechanical distortions associated with a 90°

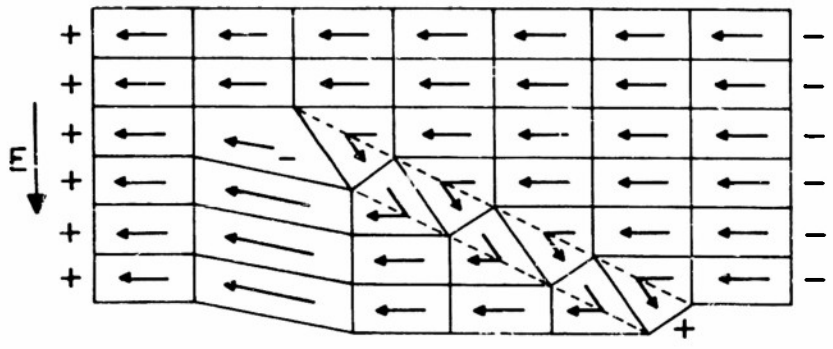

Fig. 14. Model for 90° wedge showing both mechanical and electrical distortion (exaggerated).

wedge are summarized. For reasons which will become apparent later, a crystal (called crystal "A") was chosen for the following experiments because 90° wedges were always forced out of it by stresses when the field was removed. The field required to maintain wedges in the crystal was about 1 kv/cm; it serves as a measure of the magnitude of the mechanical stresses involved. The critical field strength E_c of crystal "A" is plotted against temperature in Fig. 15 for static fields. The similarity of the E_c vs. T characteristic with that of the spontaneous polarization or the strain of a single-domain crystal as a function of temperature[10] suggests that these quantities are related.

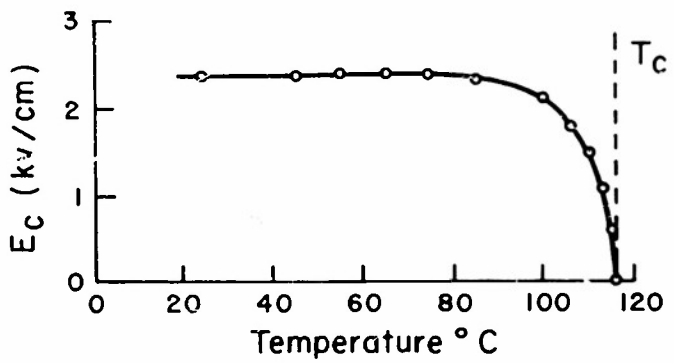

Fig. 15. Critical field for 90°-wedge nucleation as a function of temperature.

Nucleation of 90° Domains

To determine the initial growth of 90° wedges as a function of time and field strength, a square pulse was applied to single-domain crystal "A" and the number of wedges in the crystal immediately afterwards recorded. After a few minutes of rest, strain had forced the domains out and restored the single domain crystal. The number of wedges was measured as a function of pulse height E and pulse time t (Fig. 16). Each measurement at a given E and t was repeated several times; the estimated accuracy is indicated.

No wedges were ever observed for 1/4 μsec. pulses and E smaller than

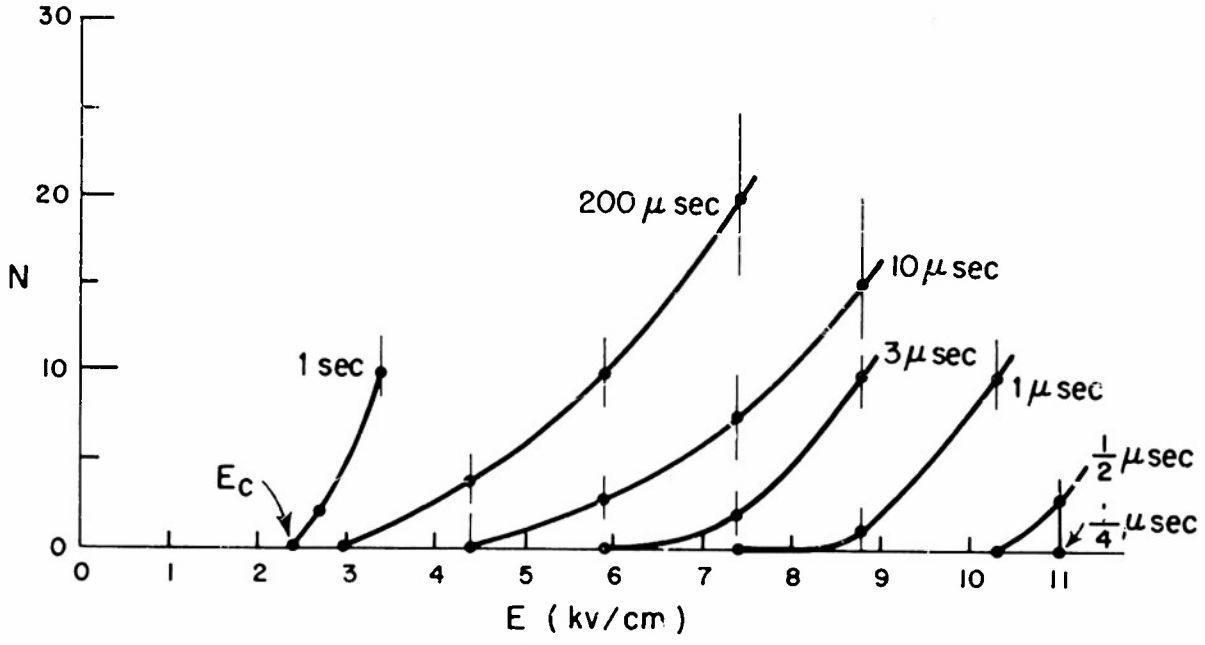

Fig. 16. Number N of 90° wedges nucleated by a square pulse as a function of pulse height and pulse length.

11 kv/cm; for pulse times longer than 1 μsec., every domain observed extended across the crystal; for times shorter than 1 μsec., some wedges did not reach across the crystal. Pulses longer than 10 μsec. widen the wedges a little after they have traversed the crystal. However, no wedges were wider than 20 μ for pulses of 200 μsec. or less. The expansion normal to the wedge axis proceeds with a velocity of about 100 cm/sec. at 7.4 kv/cm.

Figure 16 shows that N increases with E and t. It is significant that there exists a threshold pulse length, t_o, for a given field strength below which no wedges are formed. In Fig. 17, $(t_o)^{-1/2}$ is plotted against E; it appears that $t_o(E - E_c)^2$ is about a constant for low fields. Also in Fig. 17 the log of the minimum pulse length is plotted against 1/E. This curve fits best at high fields; that is, here

$$t_o = t_s e^{B/E} \qquad (2)$$

with B = 25 kv/cm and t_s = 0.05 μsec. If t_o is interpreted as the minimum time

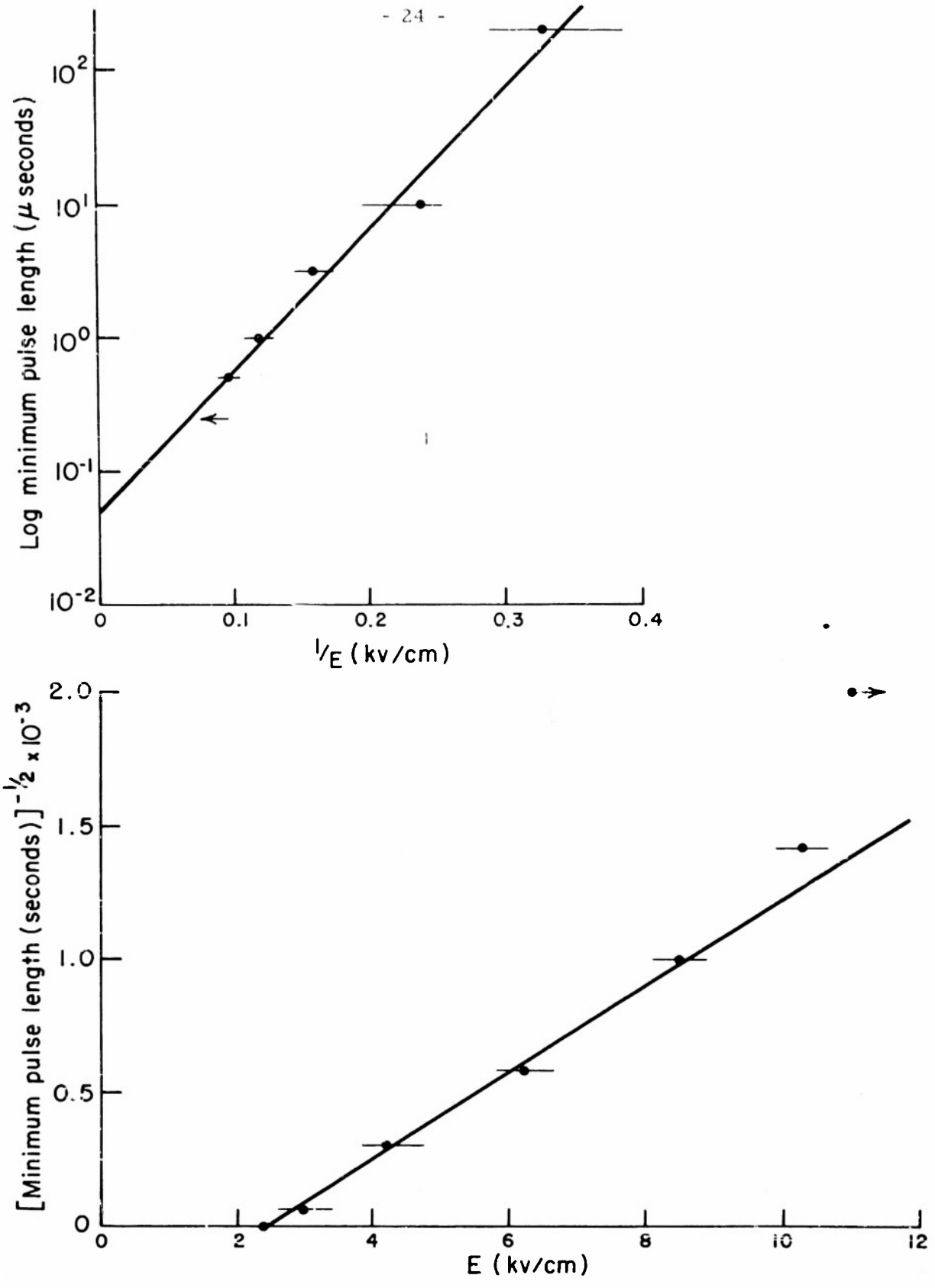

Fig. 17. Minimum pulse length t_o for nucleation of 90° wedges as a function of pulse height E.

required for 90° wedges to grow large enough to be visible, i.e., about 500 μ long, then the velocity of a wedge in the limit of high fields would be ca. 10^6 cm/sec., or the order of sound velocity.

For a given field strength, N proves in a first approximation to be proportional to $\ln (t/t_o)$. Within the accuracy of the measurements,

$$N = 0.28\, e^{\gamma E} \ln \frac{t}{t_o} \tag{3}$$

$$\frac{dN}{dt} = \frac{0.28\, e^{\gamma E}}{t} \quad , \tag{4}$$

where $\gamma = 0.36 \times 10^{-5}\ (v/m)^{-1}$. Thus the nucleation rate increases exponentially with E and decreases with 1/t. Both results appear not unreasonable. The time dependence must be visualized from the standpoint that as the domains form and grow, less material is available for the growth of new domains. Perhaps the nucleation sites become exhausted as well.

The maximum nucleation rate, at t_o, is

$$\left(\frac{dN}{dt}\right)_{max} = 5.6 \times 10^6\, e^{\gamma E}\, e^{-B/E} \left[\text{sec.}^{-1}\right] \quad . \tag{5}$$

A-C Heating

If a 60 cps a-c field is applied to crystal "A", domains are nucleated at about 2 rms kv/cm; in a high frequency field (300 kcps), the critical field for nucleation increases, as one would expect. However, before this threshold field is reached, a crystal may be heated by dielectric losses above the Curie temperature. The field required to heat our "A" crystal through the Curie point was about 5 rms kv/cm at 300 kcps. This heating effect for a crystal without domains demonstrates the large internal friction accompanying the rotation of the dipoles and the corresponding shear of the lattice.

90° Wall Motion

After 90° wedges have been introduced into a crystal, domain growth can be described in terms of wall motion. Once a wedge has grown across a crystal, the two now-parallel walls separate and move sideways with decreasing velocity and some irregularity until they stop. In crystal "A", wall motion normal to a wall for a given field strength was small. Even if the field was large enough to polarize the whole crystal in the field direction, the crystal would revert to its initial polarization when the field was removed.

For a second [100] crystal "B" such restoring forces proved appreciably smaller. After domain walls became parallel in crystal "B", not only were larger wall displacements obtained for a given field strength than in crystal "A", but if the d-c field was removed, 90° domains did not disappear from crystal "B". A comparison of the rotation of the optical axes (Fig. 18) shows that in crystal "B" the rotation was larger for a given field strength than in crystal "A". Apparently crystal "A" had a built-in strain or was slightly clamped, perhaps by the electrodes. Because of the important effects of such clamping, 90° wall motion was studied in crystal "B".

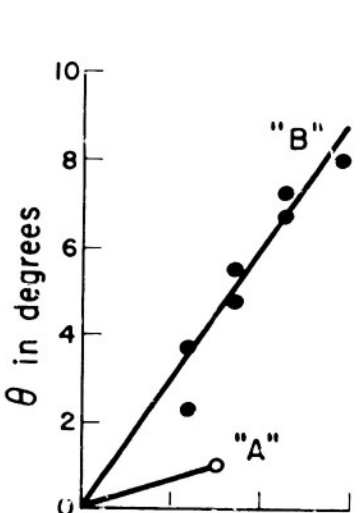

Fig. 18. Rotation of extinction direction θ as a function of field strength for crystals "A" and "B".

Since the wall velocity is zero at both extremes of an a-c oscillation, a 90° wall appears split in two at high frequencies. The distance between the two lines is designated as "wall amplitude" (Fig. 19). The wall amplitude as a function of E and frequency is plotted in Fig. 20. At 20 cps the critical field for

the onset of motion is small and the wall amplitude at low field strength approximately $\sim E^2$. The minimum field strength for wall motion increases with frequency, i.e., the wall amplitude at constant field decreases with frequency.

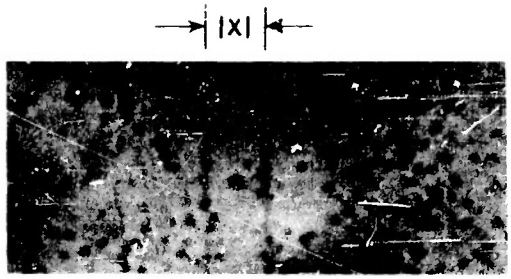

Fig. 19. 90° wall oscillating in an a-c field; frequency, 10^3 cps; wall amplitude |x| : 8.6 microns.

At 300 kcps and fields above 3.5 kv/cm, crystal "B" heats up beyond the Curie point as did crystal "A". Since temperature change affects the wall amplitude, high frequency-high field strength measurements must be viewed with caution.

The behavior of the oscillations at 300 kcps at the edge of the crystal was compared to that in the middle; no significant difference was found.

Discussion

All evidence points to the fact that a 90° wall is thick and its motion not a process of discrete molecular steps. Significant is the low critical field strength at low frequency oscillations. Depolarizing fields seem to have little effect on 90° wall motion in comparison to mechanical stress. Such stress arises because the 1° 30' deviation of the crystal axes from 90° across a wall implies that, if the wall moves, the crystal changes its shape. Conversely, when the piezo-effect changes the crystal dimensions, 90° domains must also be affected. The trend of the critical field as a function of frequency, neglecting heating effects, suggests that the wall should not be able to move at finite field strengths for frequencies much above 3 Mc. The lowest piezoelectric resonance of all our crystals was near 5 Mc. Since 90° wall motion is strongly affected by macroscopic mechanical distortions, it is not surprising to find that the wall motion is damped out as the acoustic resonance frequency is approached.

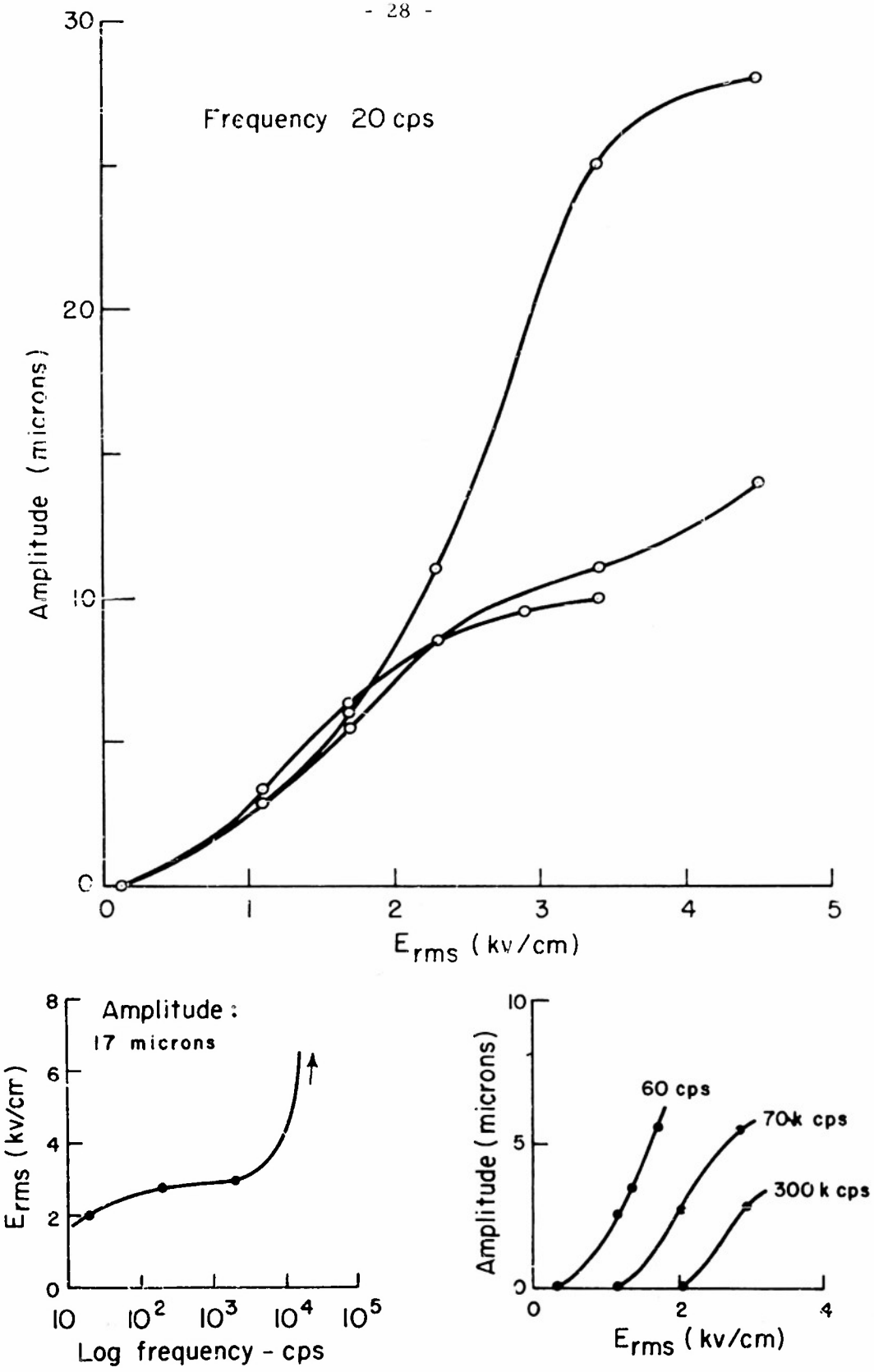

Fig. 20. 90°-wall amplitude in a-c fields as a function of frequency and field strength.

Domain Interactions

When 90° and 180° domains are simultaneously active in a crystal, a detailed interpretation of the observations obviously becomes more difficult. However, the general behavior can be predicted from a few rules most clearly demonstrated in a [101] crystal. This is the type in which we studied 180° domains (cf. Fig. 3). In a crystal with little strain, 90° and 180° domain nucleation and growth are equally favored.

Beginning our experiments with such a crystal "C" in the single-domain status, we apply a negative d-c field, and both 90° wedges and 180° wedges are formed and grow (Fig. 21). After a short time, the 180° boundaries have disappeared but the 90° walls remain. We raise the field further but produce no additional motion.

Fig. 21. 90° (and 180°) domain in a [101] crystal.

Since the 90° walls might be anchored on imperfections, we check whether or not they are bent or strained; there are no signs of strain. As we raise the field further to as high as 36 kv/cm, nothing happens except that the 90° walls become blurred and difficult to see.

The answer to this confusing situation is simple in hindsight. Through a complicated process involving 180° domains, which we shall follow in detail, the 90° walls have become head-to-head or tail-to-tail walls. That is, instead of the original head-to-tail configuration

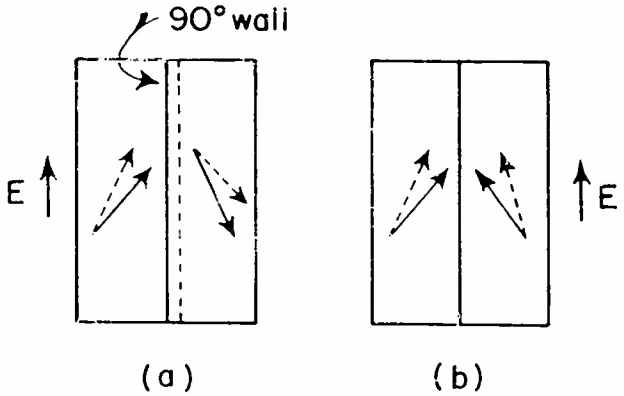

Fig. 22. Effect of field parallel to 90° wall on a) head-to-tail wall and b) head-to-head wall.

of Fig. 22a the polar axes have become reoriented as shown in Fig. 22b. As a result no force acts on the walls but only a torque on the dipoles forcing them towards the field direction. This can be verified by measuring the rotation of the extinction axes of adjacent domains; these axes rotated in opposite directions (Fig. 22b). As the field gets larger, the region near the wall rotates so far that the distortion extends over a width of about 5 μ. It appears blurred in non-polarized light but bright yellow when the rest of the crystal is near extinction.

Again, free charges at the 90° wall have neutralized the interfacial polarization that would otherwise produce a large internal field. There is no observable difference in appearance between a head-to-head, tail-to-tail, or head-to-tail wall for magnifications up to 1100 X.

A domain configuration as discussed above may be called pseudo-saturated, because, even though there exist 90° domains, they cannot be removed by a realizable field as long as the energy barrier for rotation is high. Since the magnitude of the polarization for the pseudo-saturated crystal is the same as that of a single-domain crystal, the two cases cannot be distinguished electrically.

If the field direction is reversed, 180° domains nucleate at the 90° domain boundaries and help to turn the polarization in the opposite direction. The 90° walls, which move only in the stage of head-to-tail walls, become mobilized therefore by the cooperation of 180° domains.

Wall Motion in D-C Fields

In order to understand the domain interactions, a negative d-c field with a rise time of < 0.01 sec. was applied to crystal "C". A large positive field was applied previously for several minutes to insure that the crystal was initially pseudo-saturated. The motion of a typical 90° wall, as recorded on movie film with the crystal at 45° from extinction, is plotted for two different time scales in Fig. 23(1).

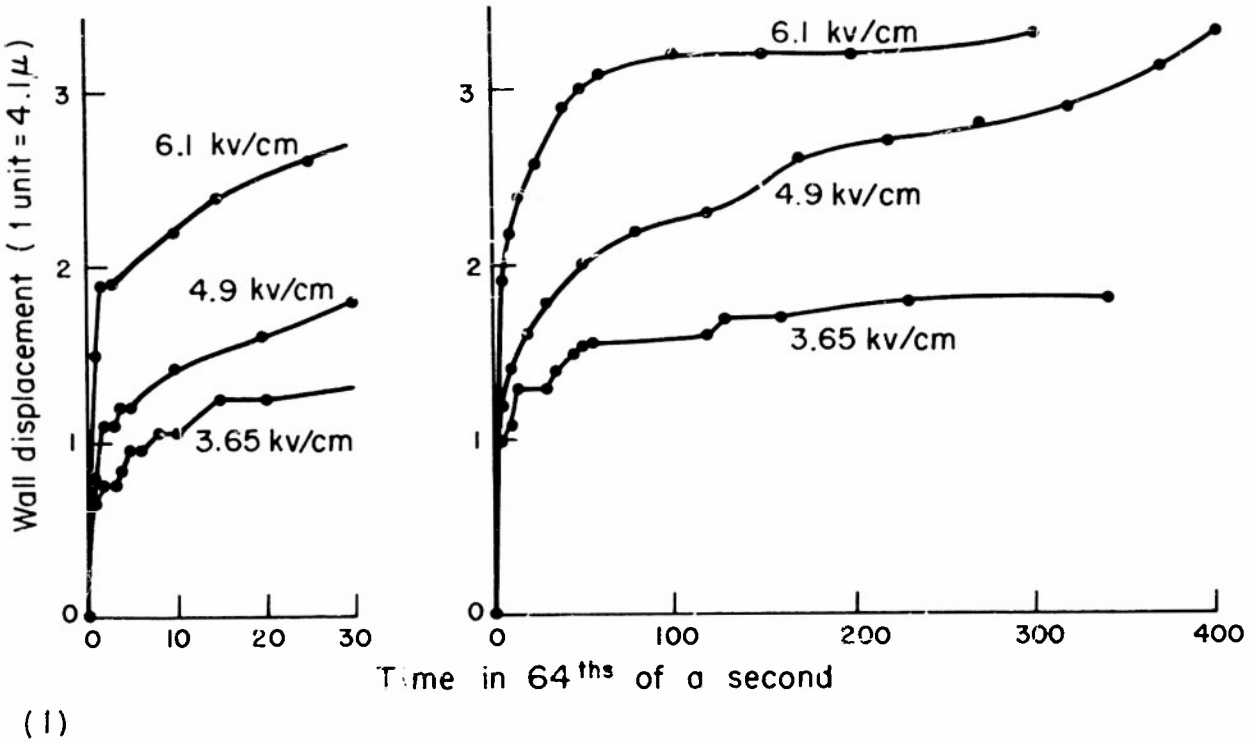

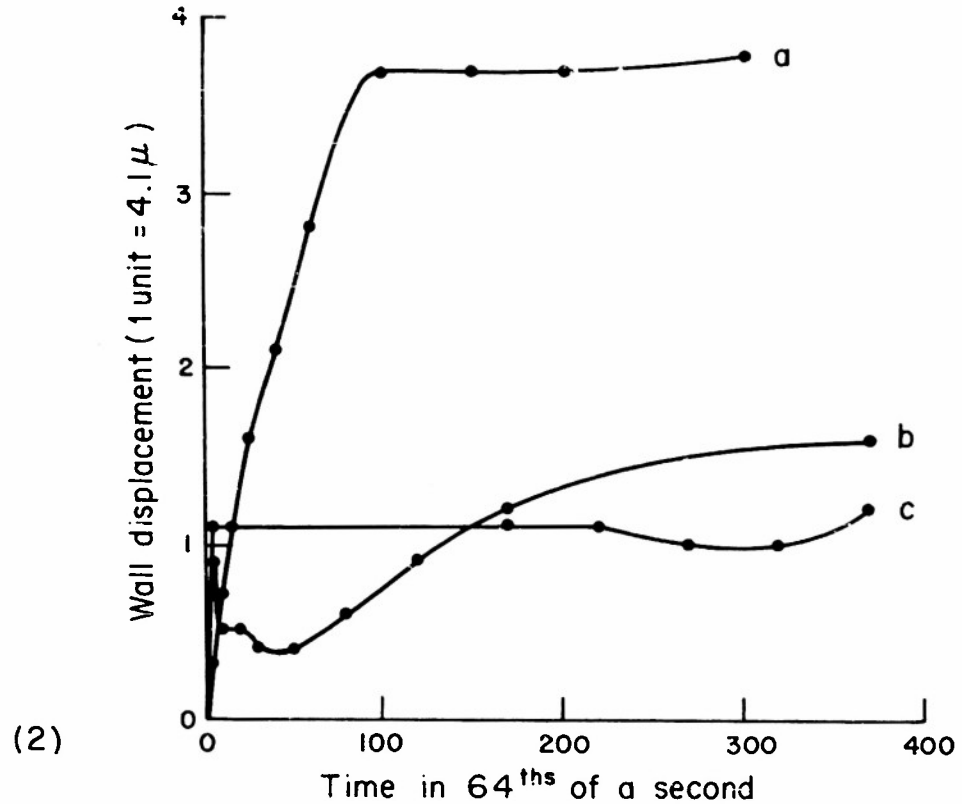

Fig. 23. 90°-wall displacement in a d-c field as a function of time. (1) represents the motion of a typical wall with two time scales. (2) shows three anomalous walls.

The significant characteristics of typical 90^{o} wall motion are that initially the velocity is very high; next the wall appears arrested for about 1/32 sec.; then it moves slowly on. The slow process nearly fits an exponential relation with a time constant of about 1/2 sec.; a better fit is provided by a relation

$$x = x_{o} \ln \frac{t}{t_{o}} \quad . \tag{6}$$

Finally there may be additional motion for times as long as 30 sec. or even several minutes.

Visual observations made at extinction show the behavior of the antiparallel domains in relation to the 90^{o} wall displacement (Fig. 24a). Since the crystal is initially pseudo-saturated, all the 90^{o} walls are head-to-head or tail-to-tail and no force acts on them when a field is first applied. If the field is just greater than the critical field for nucleation of 180^{o} domains (2 kv/cm), they will nucleate in spikes from the 90^{o} walls and proceed to slowly invert 90^{o} domains. No 90^{o} walls move. If, however, the field is greater than 2.4 kv/cm, and 180^{o} domains have nucleated, a force acts on the 90^{o} wall and it may break away from its initial position, moving freely and rapidly as a head-to-tail wall until it runs into an obstacle.

Since the location of the obstacle is a function of E, it consists probably of 180^{o} domains which are moving forward from the next 90^{o} wall. If a 90^{o} wall with an intersecting antiparallel domain is forced to move, it must shift the 180^{o} domains sideways through the crystal. This is obviously a difficult process, and the 90^{o} wall is either unable to move (Fig. 24b) or telescopes the 180^{o} domain by dragging its tip along (Fig. 24c). Both cases have actually been observed. In the first case, the 90^{o} wall was slightly bent, but still could not move. In the latter instance, a good deal of strain was observed at the 180^{o} wedge tip as it followed the 90^{o} wall. Considerations of the electrostatic fields at the 180^{o} wedge tip would lead us to expect just this behavior. Therefore the 90^{o} wall is stopped

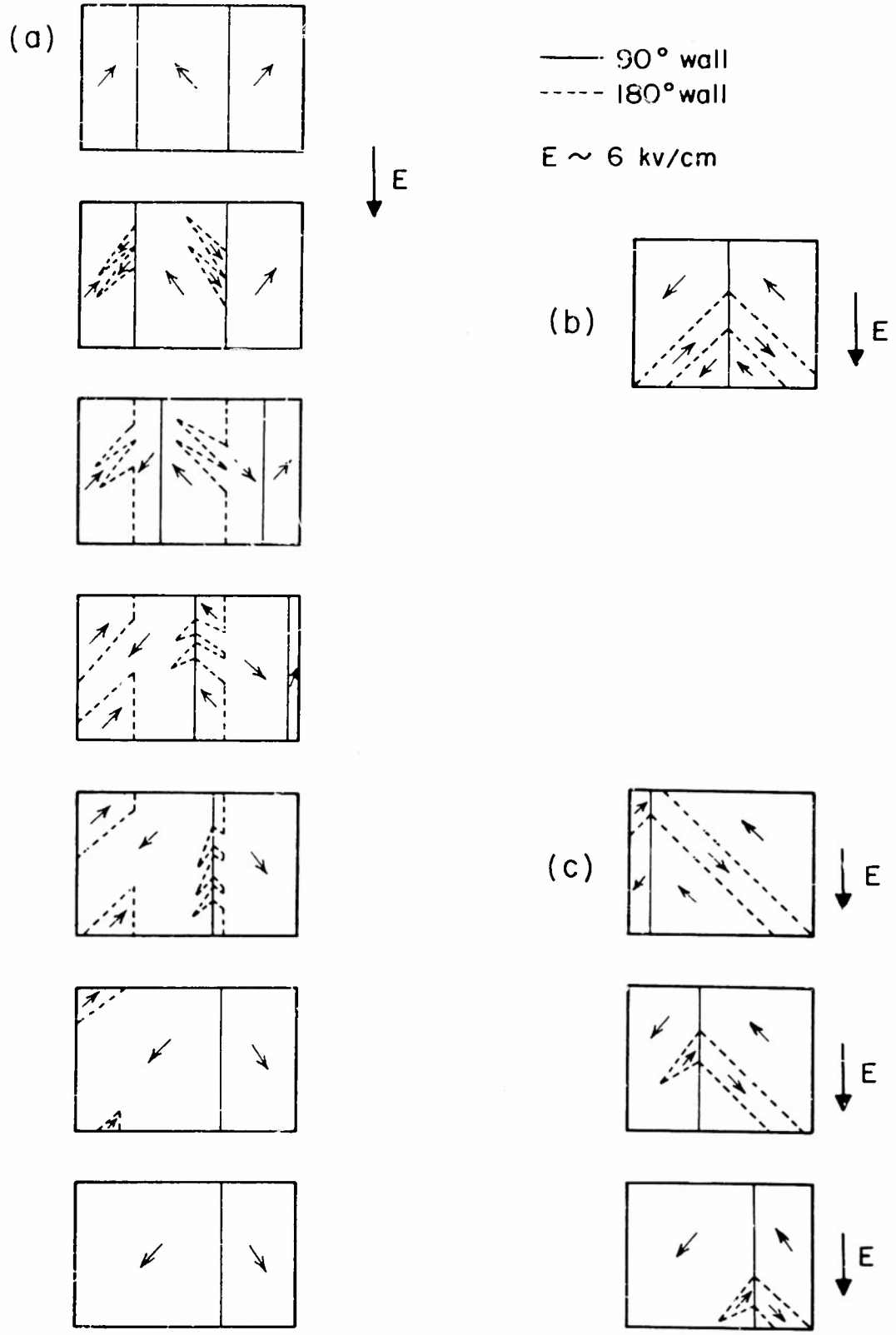

Fig. 24. 180° and 90° domain interactions in a d-c field for a [101] crystal. a) sequence of motion for a typical 90° wall; b) an anchored 90° wall; c) a 90° wall telescoping a 180° domain.

soon after it intersects 180° domains.

The subsequent slow motion (t ca. 1/2 sec.) is caused by 90° walls pushing 180° wedges. As the 180° domains grow, the area of the 90° wall on which an electric force acts decreases and the 90°-wall velocity approaches zero. Where the 90° wall comes to a stop depends on the growth rate of the 180° domains and on the field strength. Irregularities in the motion are probably due both to sudden movements or nucleations of the 180° domains and to slight imperfections in the crystal. These little jerky steps are prominently displayed in slow motion pictures and give rise to a ferroelectric Barkhausen effect.

The last part of the motion relates to the final slow disappearance of 180° domains; strain may play a part in determining the final equilibrium configuration in the field, but the end result is complete pseudo-saturation.

A particularly interesting case is displayed at the original position of the 90° wall. The electric charges left behind by the 90° wall are exactly what is needed to compensate for the interfacial polarization now arising at a 180° wall oriented at 45° to the polar axis. In other words, the head-to-head 90° wall, in order to move, had to change into a head-to-tail wall by creating a 180° wall.

Besides the case just discussed, new 90° wedges will be nucleated for fields greater than 2.4 kv/cm. A thin wedge will enter from one edge and extend across the crystal. Then the two walls will separate and, after a fast initial displacement, collide with 180° domains.

Since 180° domains can nucleate from any 90° wall on one or both sides of it, there will be a variety of cases (cf. Fig. 23(2)). Curve (a) corresponds to 180° wedges nucleated on both sides of a 90° wall. The wall therefore is never free to develop a high velocity. Case (b) probably represents a 90° wall winning out against the counteraction of 180° domains. In case (c), a 90° wall moved freely until it reached the charge residue left behind by another 90° wall. Few

or no 180° domains were nucleated in the region through which it moved. The slight rearrangement after about five seconds could be due to strain relief.

The total 90°-wall displacement during several time intervals summed over all walls as a function of E is shown in Fig. 25. The number of walls is also shown vs. E. At the larger fields, perhaps the existing walls move so fast that new wedges are absorbed before observed. All displacements are increased with E. For fields greater than 4.9 kv/cm, the region of the crystal observed is completely traversed by 90° walls (cf. Fig. 24a). This explains why the displacement approaches a limiting value at the high field strengths.

In summary, 90° and 180° domains share in the switching process. The 90° walls move in this [101] crystal because the antiparallel domains play the role of a catalyst.

Wall Motion for Square Pulses

The fast process was studied in a slightly different experiment. A negative square pulse (height 6.8 kv/cm) was applied to the initially pseudo-saturated "C" crystal. Figure 26 shows the resultant displacement summed over all 90° walls as a function of pulse length. The number of moving walls decreases with pulse length from ca. 6 at 1 sec. to ca. 1 for times below 1/100 sec. In other words, at short times only 90° walls not hampered by 180° domains move. Additional proof for this analysis comes from the observation that, if the crystal is not originally pseudo-saturated, that is, if 180° domains as well as 90° domains exist in the crystal, pulses shorter than 1/100 sec. barely move any 90° walls.

As the pulse length shortens below 10 μsec., the displacement of any wall drops rapidly to zero. A value of about 5 μ/10 μsec. (50 cm/sec.) for the sideways velocity of a free 90° wall at 6.8 kv/cm appears to describe the situation.

We conclude that 90° walls move at 50 cm/sec. until they hit the 180°

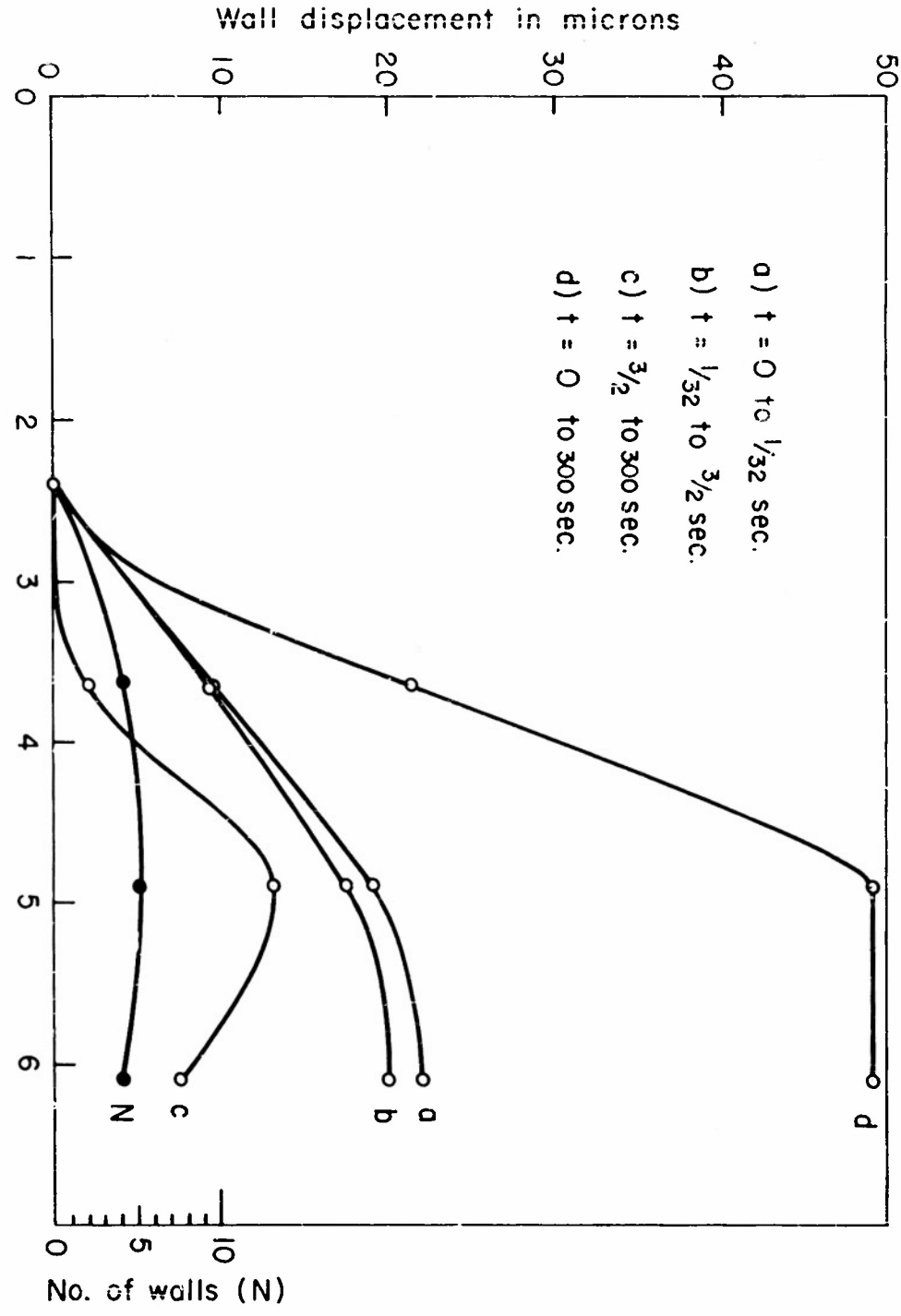

Fig. 25. Total 90°-wall displacement in a d-c field during specific time intervals as a function of field strength. The number of walls which move is also shown.

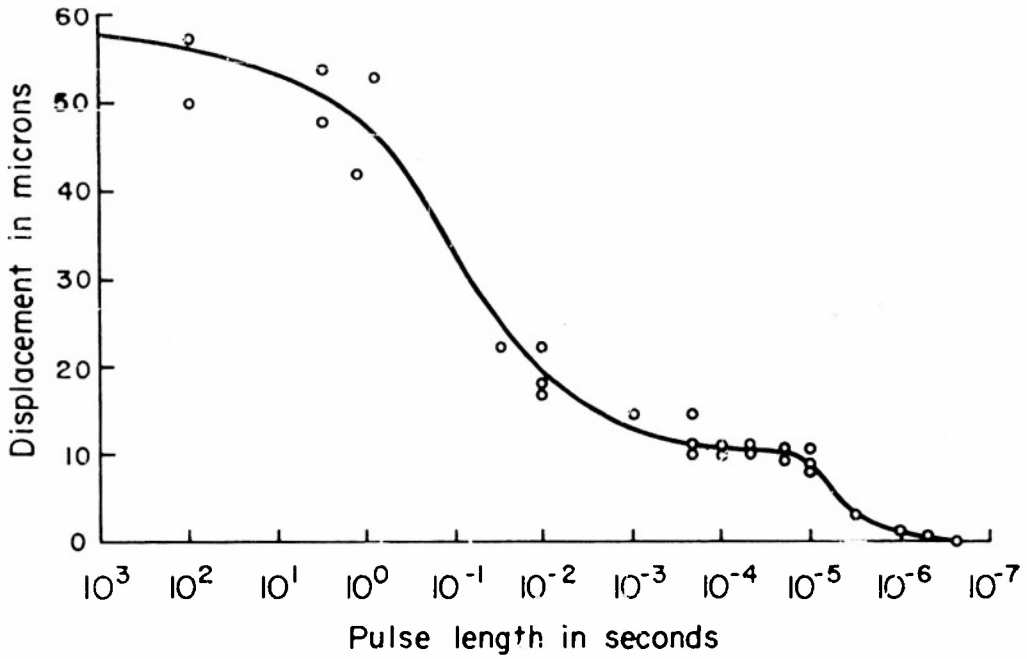

Fig. 26. Total 90°-wall displacement caused by a square pulse of height 6.3 kv/cm as a function of pulse length.

domains; then they continue with a much decreased velocity until the crystal is pseudo-saturated.

Wall Motion in A-C Fields

Figure 27 shows the frequency dependence of the 90° wall amplitude in a [101] crystal for frequencies from 10^{-2} to nearly 10^6 cps. The data were taken in the sequence a → b → c → d → e. A decrease in amplitude with increasing frequency is characteristic of a free 90° wall. The dependence of the wall amplitude on time and prehistory (as well as the existence of a large critical field for motion) are characteristic of a 90° wall which interacts with 180° domains.

Temperature Effects

Figure 28 shows the 90° wall amplitude at 60 cps as a function of temperature in a [101] crystal for several field strengths. The amplitude goes through

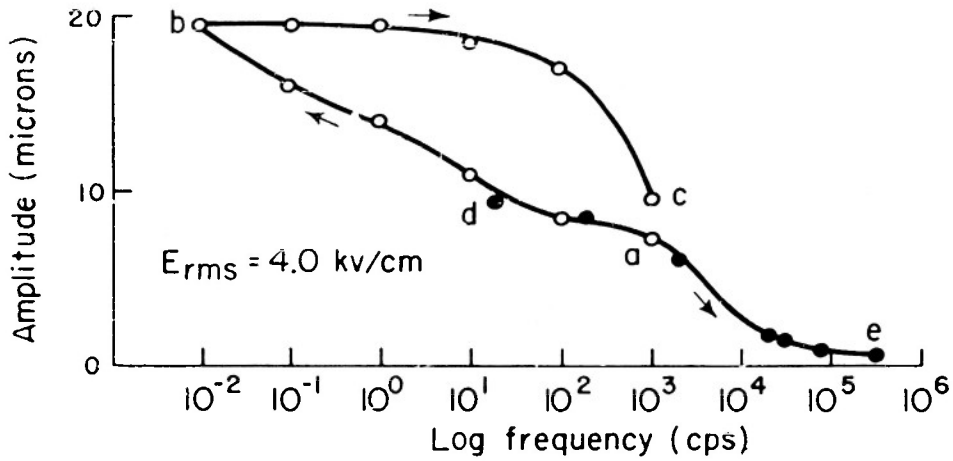

Fig. 27. 90°-wall amplitude as a function of frequency for a [10i] crystal.

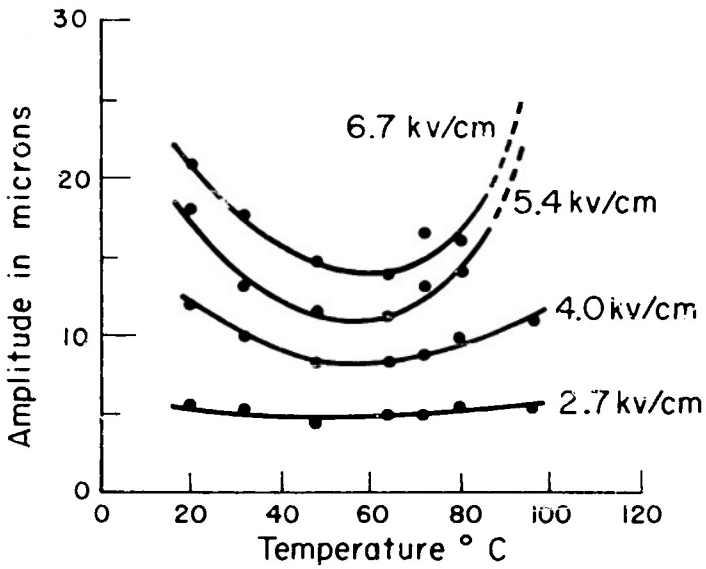

Fig. 28. Dependence of 90°-wall amplitude on temperature in a 60 cycle a-c field.

a slight minimum near 60°C as the temperature increases from room temperature to about 100°C. At temperatures above 80°C, the number of 90° domains suddenly increases tremendously (Fig. 29). Double-ended wedges nucleate in the body

of the crystal and the domain walls often become too dense for counting. These effects are most prominent at high field strengths. This abundance of 90° domains, which makes it difficult to study other temperature effects in our crystals, appears to be caused by the lowering of the energy barrier for rotation (Appendix) and a decrease in the 90° wall energy at high temperatures. Less than 10°C below the Curie point, the wall energy is apparently so small that a 90° wall can bend as much as 4° from its original (101) plane. The wall at high temperatures appears nearly isotropic, i.e., black in polarized light but transparent and hard to see in unpolarized light.

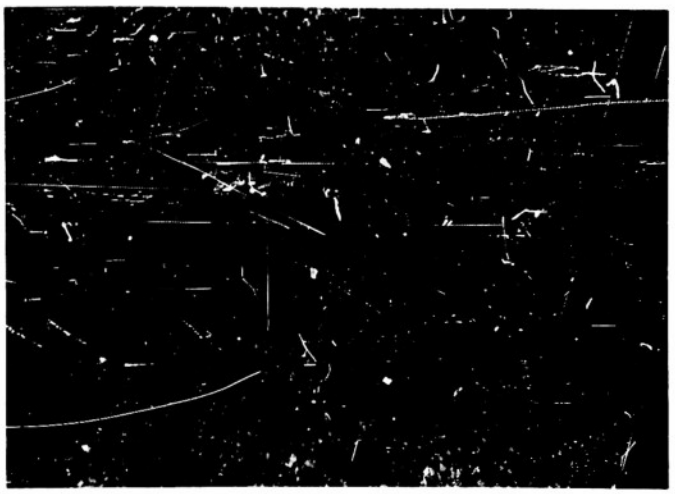

Fig. 29. 90° domain which appears in a [101] crystal if a field is applied at a temperature above 80°C.

Acknowledgments

The author wishes to express her appreciation to Professor A. R. von Hippel for suggesting the problem and for his advice and encouragment during the course of this research. She also wishes to thank Dr. P. W. Forsbergh, Jr,, for an introduction to the intricacies of domain patterns in barium titanate crystals and for many illuminating discussions. Gratitude is expressed to Professor F. R. Kotter for the use of his rectangular pulse generator and to Professor H. E. Edgerton for the use of a stroboscopic light. The assistance of W. B. Westphal in obtaining the dielectric measurements, and of L. E. Johnson, B. Frackiewics, and Professor D. J. Epstein in the electrical instrumentation is

gratefully acknowledged.

The author is indebted to the International Business Machines Corp. for support in the form of a fellowship, and to Dr. D. R. Young of I.B.M. for many informative discussions.

APPENDIX

Free Energy for Rotation of the Polar Axis

The free energy for a single domain of tetragonal barium titanate at zero stress compared to the free energy of the cubic configuration is given[16] as a function of polarization (considering only rotation of the polar axis in the xz plane);

$$A(\underset{\rightarrow}{P}) = D_1(P_x^2 + P_z^2) + D_2(P_x^4 + P_z^4) + D_3(P_x^6 + P_z^6) + D_4 P_x^2 P_z^2 \quad . \qquad (7)$$

Merz[24] has determined from measurements in the z direction that

$$D_1 = 3.7\times10^{-5}(T - T_o); \quad D_2 = 1.7\times10^{-13}; \quad D_3 = 3.8\times10^{-23} \ \left[\text{cgs-esu}\right] . \qquad (8)$$

T_o is the Curie-Weiss temperature.

D_4 may be determined from the equation

$$\frac{\partial^2 A}{\partial P_x^2} = \frac{1}{\epsilon_a} = 2(D_1 + D_4 P_z) \quad , \qquad (9)$$

where $P_x = 0$ and $P_z = P_s$. Another way is to vary D_4 in Eq. (7) until the free energy of the tetragonal phase equals the free energy of the orthorhombic phase at 0°C. Both methods give $D_4 = 6(\pm 1) \times 10^{-13}$ cgs-esu, but the second method, being internally consistent, is preferred. We will use the value $D_4 = 5.9\times10^{-13}$ cgs-esu. The exact shape of the calculated curves which follow is very sensitive to D_1, D_2, D_3, and D_4.

Changing to polar coordinates, let 0 be the angle between the polar axis and the c axis. Let P_s' be defined as the value of P for which $\frac{\partial A(P,\theta)}{\partial P} = 0$.

24) W. J. Merz, Phys. Rev. 91, 513 (1953).

In Figure 30 we plot P_s' against θ for several temperatures. P_s' is independent of θ for temperatures near 50°C, but for temperatures above 80°C, P_s' decreases rapidly as θ goes from 0° to 45°.

Figure 31a shows $A(P, 0^\circ)$. The minimum obviously occurs at $P = P_s$. In Figure 31b, $A(P_s', \theta)$ is plotted against θ for several temperatures. At high temperatures, the barrier for rotation by 90° decreases. On the other hand, as the temperature is lowered below 25°C, a metastable minimum develops at 45° which, below 0°C, becomes the lowest energy configuration (orthorhombic phase).

Simplified Free Energy for Rotation

It can be shown that there is one temperature, 55°C, at which P_s' is independent of θ. From Eq. (7) it follows rigorously that if P_s' is independent of

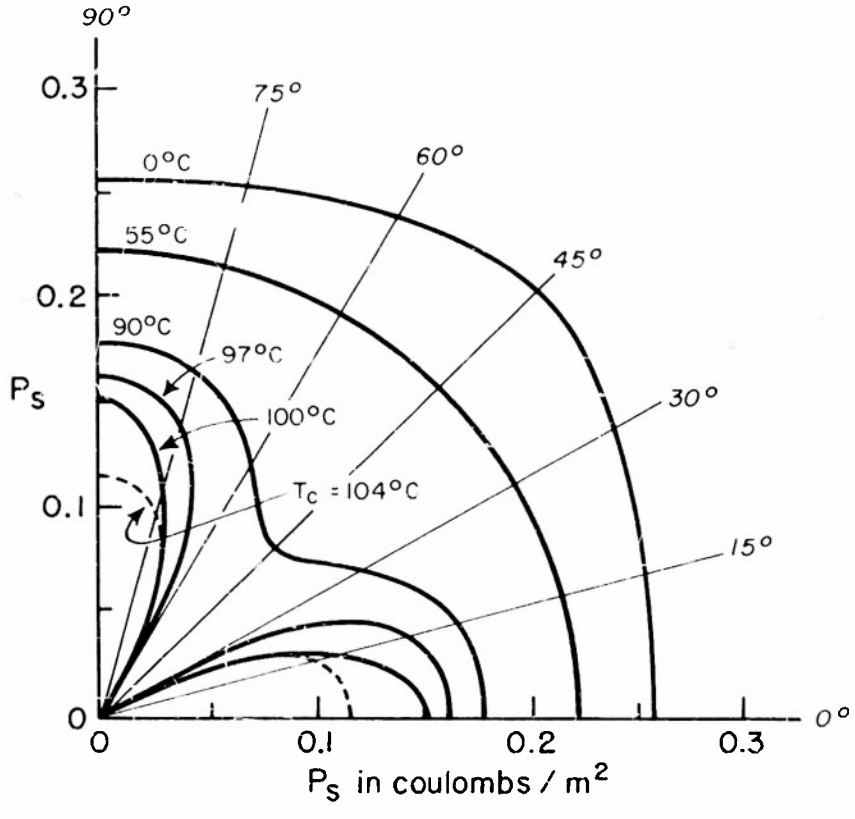

Fig. 30. Polar plot of P_s' as a function of θ.

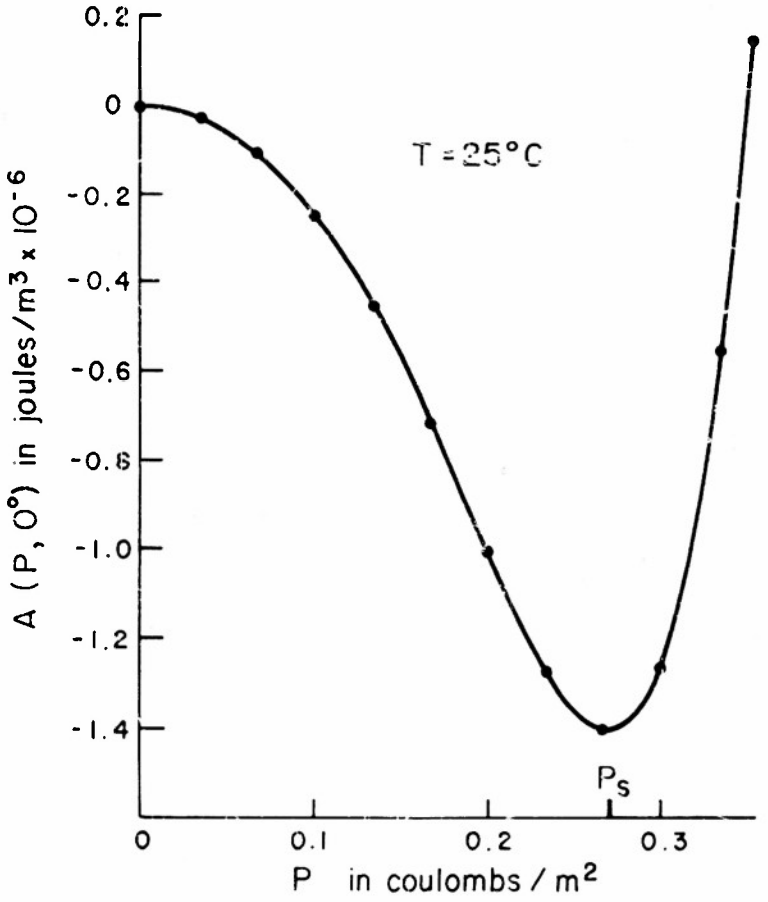

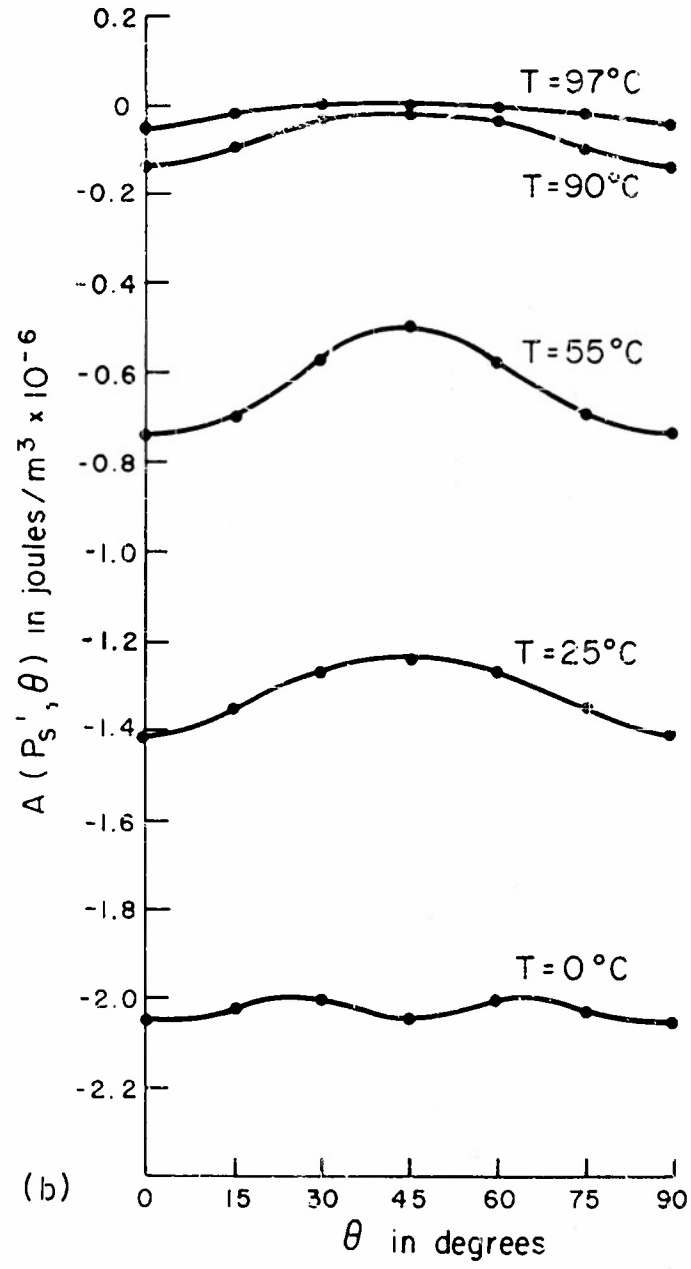

Fig. 31. Free energy A(P, θ): (a) A(P, 0°) as a function of P; (b) A(P_s', θ) as a function of θ.

θ, then

$$A = P_s K \sin^2 \theta \cos^2 \theta + K_o, \tag{10}$$

where K_o does not depend on θ. Since this equation is simple analytically and is correct for a temperature near room temperature, we may use it as a first approximation of behavior at room temperature. Fitting Eq. (10) to the curve of $A(P_s', \theta)$ at 25°C, we find $K \sim 25$ kv/cm.

90° Wall Energy

Let us assume that, since the wall is thick, the dipole moment is constant and the dipole angle, θ, varies continuously and linearly through the wall, i.e., $\frac{d\theta}{dx} = \frac{\pi/2}{d}$ from $\theta = 0$ at $x = 0$ to $\theta = \frac{\pi}{2}$ at $x = d$, where d is the wall thickness. We will also assume that the mechanical deformation which is prescribed for each θ at zero stress is realized. For a stationary wall, free charge will neutralize any divergence of P. With the above assumptions, the energy density in a small volume in the wall will be $u_1 = P_s K \sin^2 \theta \cos^2 \theta$, plus an additional term, u_2, to account for the variation in θ through the wall. The wall energy per unit area, σ_{90^o}, will then be the sum of two terms, σ_{u_1} and σ_{u_2}, where

$$\sigma_{u_1} = \frac{2}{\pi} K P_s d \int_o^{\pi/2} \sin^2 \theta \cos^2 \theta \, d\theta = \frac{K P_s d}{8} \quad . \tag{11}$$

σ_{u_1} will be a minimum if the wall is thin. Since u_2 must represent a force tending to align the dipoles, σ_{u_2} will be lower for a thick wall. Let us postulate an energy of the form

$$\sigma_{u_2} = \frac{b\pi^2}{4ad} \quad , \tag{12}$$

where b is a constant, and a the lattice spacing 4A°. Then

$$\sigma_{90^o} = \frac{K P_s d}{8} + \frac{b\pi^2}{4ad} \quad . \tag{13}$$

Now σ_{90^o} will be a minimum when $\frac{\partial \sigma_{90^o}}{\partial d} = 0$ which gives

$$b = \frac{d^2 K P_s a}{2\pi^2} \tag{14}$$

Therefore

$$\sigma_{90^\circ} = \frac{K P_s d}{4} \quad , \tag{15}$$

which for K = 25 kv/cm, P_s = 0.26 coul/m^2 and d = 0.4 microns, gives

$$\sigma_{90^\circ} \simeq 6.5 \times 10^{-2} \quad \left[\text{joules/m}^2\right] \quad . \tag{16}$$